Appendix A:

Miller Indices

(Nix, 2002)

5.2.1 Surface Structure of Metals

In most technological applications, metals are used either in a finely divided form (e.g. supported metal catalysts) or in a massive, polycrystalline form (e.g. electrodes, mechanical fabrications). At the microscopic level, most materials, with the notable exception of a few truly amorphous specimens, can be considered as a collection or aggregate of single crystal crystallites. The surface chemistry of the material as a whole is therefore crucially dependent upon the nature and type of surfaces exposed on these crystallites. *In principle*, therefore, the surface properties of any material may be understood if

1. the amount of each type of surface exposed is known, and
2. detailed knowledge of the properties of each and every type of surface plane is available.

(This approach assumes that the possible influence of crystal defects and solid state interfaces on the surface chemistry may be neglected)
It is therefore vitally important to study different, well-defined surfaces independently. The most commonly employed technique is to prepare macroscopic (i.e. size ~ cm) single crystals of metals and then to deliberately cut them in a way which exposes a large area of the specific surface of interest.

Most metals only exist in one bulk structural form - the most common metallic crystal structures being:

bcc	**Body-centred cubic**
fcc	**Face-centred cubic**
hcp	**Hexagonal close packed**

For each of these crystal systems, there are in principle an infinite number of possible surfaces which can be exposed. In practice, however, only a limited number of planes (predominantly the so-called "low-index" surfaces) are found to exist in any significant amount and attention is thus focussed on these surfaces. Furthermore, it is possible to predict the ideal atomic arrangement at a given surface of a particular metal by considering how the bulk structure is intersected by the surface. Firstly, however, look in detail at the bulk crystal structures.

I. The *hcp* and *fcc* structures

The *hcp* and *fcc* structures are closely related: they are both based upon stacking layers of atoms, where the atoms are arranged in a close-packed hexagonal manner within the individual layer.

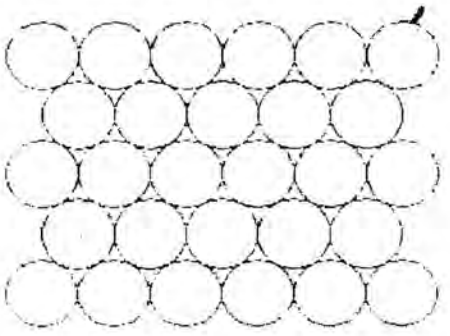

Figure A1. First layer of hcp and fcc structures

The atoms of the next layer of the structure will preferentially sit in some of the hollows in the first layer - this gives the closest approach of atoms in the two layers.

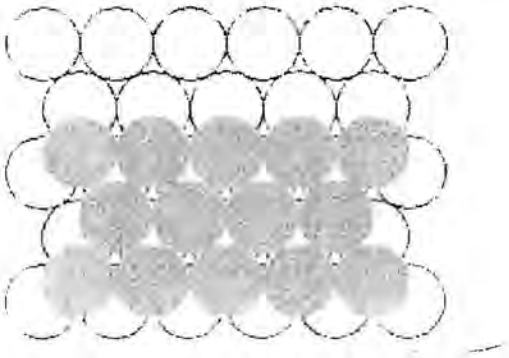

Figure A2. Second layer atoms of hcp and fcc structures

When it comes to deciding where the next layer of atoms should be positioned there are two choices - these differ only in the relative positions of atoms in the 1st and 3rd layers.

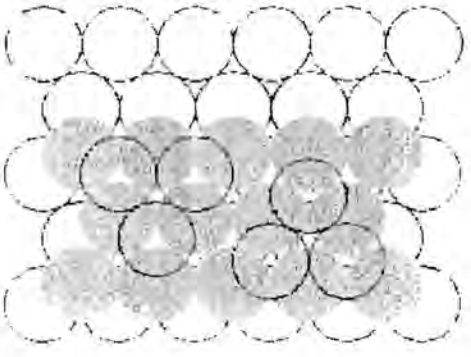

In the structure on the left the atoms of the 3rd layer sit directly above those in the 1st layer - this gives rise to the characteristic. ABABA. packing sequence of the hcp structure.
In the structure on the right of the last figure on the previous page the atoms of the 3rd layer are laterally offset from those in both the 1st and 2nd layers, and it is not until the 4th layer that the sequence begins to repeat. This is the ..ABCABC.. packing sequence of the fcc structure.
Because of their common origin, both of these structures share common features:

1. The atoms are close packed
2. Each atom has 12 nearest neighbours (i.e. CN = 12)

(a) *fcc* structure

Although it is not immediately obvious, the ..ABCABC.. packing sequence of the *fcc* structure gives rise to a three-dimensional structure with cubic symmetry (hence the name !).

fcc structure

Figure A3. The fcc structure

It is the cubic unit cell that is commonly used to illustrate this structure - but the fact that the origin of the structure lies in the packing of layers of hexagonal symmetry should not be forgotten.

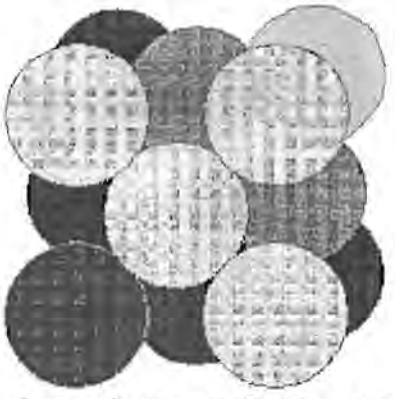

Figure A4. Different layers hexagonally close packed

The above diagram shows the atoms of one of the hexagonal close-packed layers highlighted in shades of grey (except for the top right corner atom), and the atoms of another highlighted in black.

(b) *hcp* structure

The ..ABABA.. packing sequence of the *hcp* structure gives rise to a three-dimensional unit cell structure whose symmetry is more immediately related to that of the hexagonally-close packed layers from which it is built, as illustrated in the diagram below.

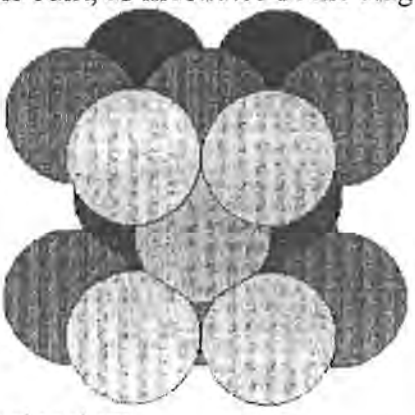

Figure A5. The hcp structure

II. The *bcc* structure

The *bcc* structure has very little in common with the *fcc* structure - except the cubic nature of the unit cell. Most importantly, it differs from the *hcp* and *fcc* structures in that it is not a close-packed structure.

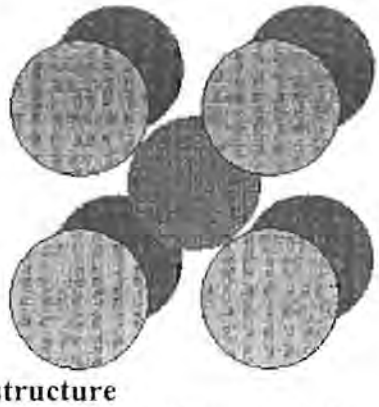

bcc structure

Figure A6. The bcc structure

The bulk co-ordination number of atoms in the bcc structure is 8

Rationale

Consider the atom at the centre of the unit cell as it is conventionally drawn. The nearest neighbours of this atom are those at the corners of the cube which are all equidistant from the central atom. There are eight such corner atoms so the CN of the central atom (and all atoms in the structure) is eight.

Whereto from here?

An ordered surface may be obtained by cutting the three-dimensional bulk structure of a solid along a particular plane to expose the underlying array of atoms. The way in which this plane intersects the three-dimensional structure is very important and is defined by using Miller Indices this notation is commonly used by both surface scientists and crystallographers since an *ideal*

surface of a particular orientation is nothing more than a lattice plane running through the 3D crystal with all the atoms removed from one side of the plane.
In order to see what surface atomic structures are formed on the various Miller index surfaces for each of the different crystal systems consider how the lattice planes bisect the three-dimensional atomic structure of the solid. As it might be expected, however, the various surfaces exhibit a wide range of:

1. Surface symmetry
2. Surface atom co-ordination , and most importantly this results in substantial differences in : 3) and 4)
3. Physical properties (electronic characteristics etc.), and
4. Surface chemical reactivity (catalytic activity, oxidation resistance etc.)

5.2.2 Surface Structure of fcc Metals

Many of the technologically most important metals possess the fcc structure: for example the catalytically important precious metals (Pt, Rh, Pd) all exhibit an fcc structure.
The low index faces of this system are the most commonly studied of surfaces: they exhibit a range of

1. **Surface symmetry**
2. **Surface atom co-ordination**
3. **Surface reactivity**

I. The fcc (100) surface

The (100) surface is that obtained by cutting the fcc metal parallel to the front surface of the fcc cubic unit cell - this exposes a surface (the atoms in the darkest colour) with an atomic arrangement of 4-fold symmetry

Figure A7. The fcc (100) surface

The diagram in figure A8 shows the conventional birds-eye view of the (100) surface - this is obtained by rotating the preceding diagram through 45° to give a view which emphasises the 4-fold symmetry of the surface layer atoms.

Figure A8. Birds-eye view of the fcc(100) surface
The tops of the second layer of atoms are just visible through the holes in the first layer, but would not be accessible to molecules arriving from the gas phase. The co-ordination number of the atoms on the surface is 8.

There are several other points worthy of note :

1. All the surface atoms are equivalent
2. The surface is relatively smooth at the atomic scale
3. The surface offers various adsorption sites for molecules which have different local symmetries and lead to different co-ordination numbers :
    - On-top sites (CN=1)
    - Bridging sites, between two atoms (CN=2)
    - Hollow sites, between four atoms (CN=4)

(In the above context, the CN is taken to be the number of surface metal atoms to which the adsorbed species would be directly bonded)

II. The fcc(110) surface

fcc unit cell
(110) face

Figure A9. The fcc (110) surface
The (110) surface is obtained by cutting the fcc unit cell in a manner that intersects the x and y axes but not the z-axis - this exposes a surface with an atomic arrangement of 2-fold symmetry. The next diagram shows the conventional birds-eye view of the (110) surface - emphasising the rectangular symmetry of the surface layer atoms. The diagram has been rotated such that the rows of atoms in the first atomic layer now run vertically, rather than horizontally as in the previous diagram.

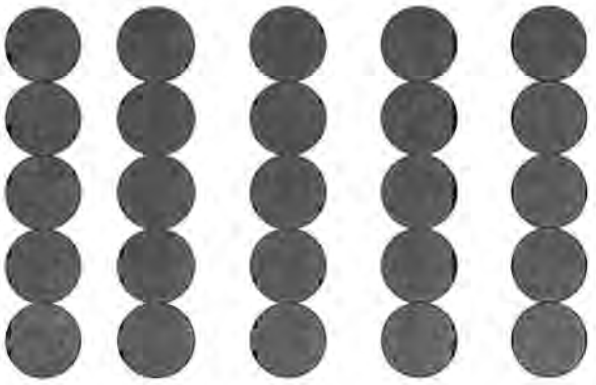

Figure A10. Atoms in topmost layer

It is clear from this view that the atoms of the topmost layer are much less closely packed than on the (100) surface - in one direction (along the rows) the atoms are in contact i.e. the distance between atoms is equal to twice the metallic (atomic) radius, but in the orthogonal direction there is a substantial gap between the rows.

This means that the atoms in the underlying second layer are also, to some extent, exposed at the surface

(110) surface plane
e.g. Cu(110)

Figure A11. The fcc (110) surface plane

The preceding diagram illustrates some of those second layer atoms, exposed at the bottom of the troughs.

In this case, the determination of co-ordination numbers requires a little more careful thought: one way to double-check the answer is to remember that the CN of atoms in the bulk of the fcc structure is 12, and then to subtract those which have been removed from above in forming the surface plane.

If one compares this co-ordination number (CN = 7) with that obtained for the (100) surface, it is worth noting that the surface atoms on a more open ("rougher") surface have a lower CN - this has important implications when it comes to the **chemical reactivity** of surfaces.

The fact that they are clearly exposed (visible) at the surface implies that they have a lower CN than they would in the bulk.

In summary, we can note that

1. All first layer surface atoms are equivalent, but second layer atoms are also exposed
2. The surface is atomically rough, and highly anisotropic
3. The surface offers a wide variety of possible adsorption sites, including :
    - On-top sites (CN=1)
    - Short bridging sites between two atoms in a single row (CN=2)
    - Long bridging sites between two atoms in adjacent rows (CN=2)
    - Higher CN sites (in the troughs)

III. The fcc (111) surface

The (111) surface is obtained by cutting the fcc metal in such a way that the surface plane intersects the x-, y- and z- axes at the same value - this exposes a surface with an atomic arrangement of 3-fold (apparently 6-fold, hexagonal) symmetry. This layer of surface atoms actually corresponds to one of the close-packed layers on which the fcc structure is based.

fcc unit cell
(111) face

Figure A12. The fcc unit cell (111) face

The diagram below shows the conventional birds-eye view of the (111) surface - emphasising the hexagonal packing of the surface layer atoms. Since this is the most efficient way of packing atoms within a single layer, they are said to be "close-packed".

(111) surface plane
e.g. Pt(111)

Figure A13. The fcc (111) surface plane

The following features are worth noting;

1. All surface atoms are equivalent and have a relatively high CN
2. The surface is almost smooth at the atomic scale

3. The surface offers the following adsorption :
    - On-top sites (CN=1)
    - Bridging sites, between two atoms (CN=2)
    - Hollow sites, between three atoms (CN=3)

IV. How do these surfaces intersect in irregular-shaped samples?
Flat surfaces of single crystal samples correspond to a single Miller Index plane and it was seen that, each individual surface has a well-defined atomic structure. It is these flat surfaces that are used in most surface science investigations, but it is worth a brief aside to consider what type of surfaces exist for an irregular shaped sample (but one that is still based on a single crystal). Such samples can exhibit facets corresponding to a range of different Miller Index planes.

SUMMARY
Depending upon how an fcc single crystal is cleaved or cut, flat surfaces of macroscopic dimensions which exhibit a wide range of structural characteristics may be produced.
The single crystal surfaces discussed here ((100), (110) & (111)) represent only the most frequently studied surface planes of the fcc system - however, they are also the most commonly occurring surfaces on such metals and the knowledge gained from studies on this limited selection of surfaces goes a long way in propagating the development of our understanding of the surface chemistry of these metals.

5.2.3 Surface Structure of hcp Metals

This important class of metallic structures includes metals such as Co, Zn, Ti & Ru.
The Miller Index notation used to describe the orientation of surface planes for all crystallographic systems is slightly more complex in this case since the crystal structure does not lend itself to description using a standard Cartesian set of axes- instead the notation is based upon three axes at 120 degrees in the close-packed plane, and one axis (the c-axis) perpendicular to these planes. This leads to a four-digit index structure; however, since the third of these is redundant it is sometimes left out!

I. The hcp (0001) surface
This is the most straightforward of the hcp surfaces since it corresponds to a surface plane which intersects only the c-axis, being coplanar with the other 3 axes i.e. it corresponds to the close packed planes of hexagonally arranged atoms that form the basis of the structure. It is also sometimes referred to as the (001) surface.

(0001) surface plane
e.g. Ru(0001)

Figure A14.The hcp (0001) surface plane

This conventional plan view of the (0001) surface shows the hexagonal packing of the surface layer atoms. This is very similar to the fcc(111) surface.

We can summarise the characteristics of this surface by noting that:

1. All the surface atoms are equivalent and have CN=9
2. The surface is almost smooth at the atomic scale
3. The surface presents adsorption sites which are locally :
    - On-top sites (CN=1)
    - Bridging sites, between two atoms (CN=2)
    - Hollow sites, between three atoms (CN=3)

5.2.4 Surface Structure of bcc Metals

A number of important metals (e.g. Fe, W, Mo) have the bcc structure. As a result of the low packing density of the bulk structure, the surfaces also tend to be of a rather open nature with surface atoms often exhibiting rather low co-ordination numbers.

I. The bcc (100) surface

Figure A15. The bcc unit cell (100) face

bcc unit cell
(100) face

The (100) surface is obtained by cutting the metal parallel to the front surface of the bcc cubic unit cell - this exposes a relatively open surface with an atomic arrangement of 4-fold symmetry. The diagram below shows a plan view of this (100) surface - the atoms of the second layer (shown on left) are clearly visible, although probably inaccessible to any gas phase molecules other than smaller atoms or molecules like N_2, H_2 or ions that result during cutting.

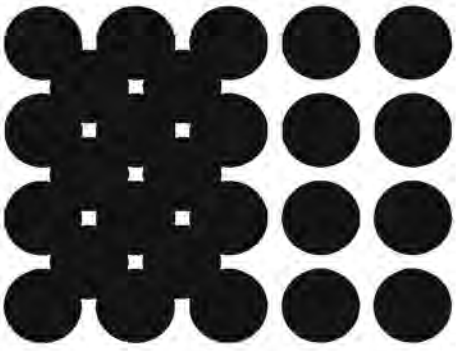

bcc (100) surface plane
e.g. Fe(100)

Figure A16. The bcc(100) surface plane

The co-ordination number for the surface atoms is 4. The nearest neighbours are at a distance of 0.87a.

The CN of metal atoms in the bulk of the solid is 8 for a bcc metal and the second layer of atoms clearly have 4 nearest neighbours in the 1st layer and another 4 in the 3rd layer.

II. The bcc (110) surface

The (110) surface is obtained by cutting the metal in a manner that intersects the x and y axes but creates a surface parallel to the z-axis - this exposes a surface that has a higher atom density than the (100) surface.

bcc unit cell
(110) face

Figure A17. The bcc unit cell (110) face

Figure A18 shows a plan view of the (110) surface - the atoms in the surface layer strictly form an array of rectangular symmetry, but the surface layer co-ordination of an individual atom is quite close to hexagonal.

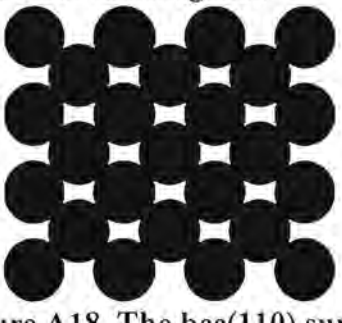

bcc(110) surface plane
e.g. Fe(110)

Figure A18. The bcc(110) surface plane

The co-ordination number of the surface layer of atoms is 6. Think in 3 dimensions.

Rationale

Each surface atom has four nearest neighbours in the 1st layer (the remaining two "near-neighbours" in this surface layer being at a slightly greater distance), but there are also two nearest neighbours in the layer immediately below.

III. The bcc (111) surface

The (111) surface of bcc metals is similar to the (111) face of fcc metals only in that it exhibits a surface atomic arrangement exhibiting 3-fold symmetry - in other respects it is very different.

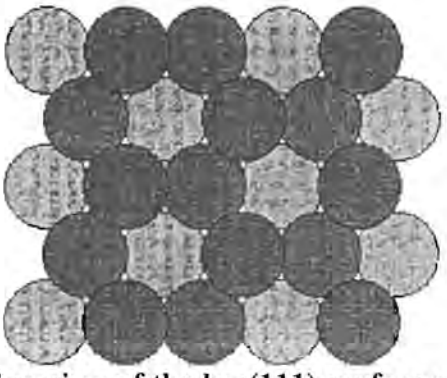

Top View:
bcc(111) surface plane
e.g. Fe(111)

Figure A19. Top view of the bcc(111) surface plane

In particular it is a very much more open surface with atoms in both the second and third layers clearly visible when the surface is viewed from above. This open structure is also clearly evident when the surface is viewed in cross-section as shown in figure A20 in which atoms of the various layers have been annotated.

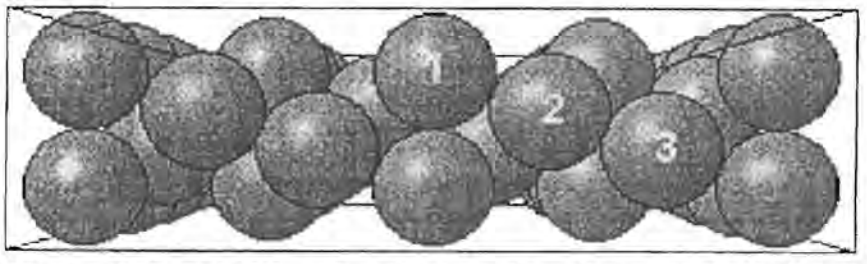

Figure A20. Side View: bcc(111) surface plane e.g. Fe(111)

Appendix B:

The aluminium alloys are given a letter designation to indicate the processes that they have been through prior to resulting in the plate, sheet or extrusion.
The designations are as follows: (Follette, 1980)

- O - annealed wrought aluminium
- F - as cast or as fabricated
- H - cold worked
- T - heat treated

The T group indicates heat treated aluminium alloys and the Table A2.1 indicates the type of heat treatment.

T2	Annealed for ductility and dimensional stability (Cast only)
T3	Heat treated and cold worked. (Wrought only)
T4	Heat treated and naturally aged to stability. (Wrought or cast)
T5	Artificially aged. (Wrought or cast)
T6	Heat treated and artificially aged. (Wrought or cast)
T7	Heat treated and stabilised. (Cast only)
T8	Heat treated, cold worked, and artificially aged. (Wrought only)
T9	Heat treated, artificially aged, and cold worked. (Wrought only)
T10	Artificially aged, and cold worked. (Wrought only)

Table A2.1 Type of heat treatments for aluminium alloys.

As the number increases the hardness increases.

Heat-Treatable Al-Si-Mg Wrought Alloy 6082

Chemical Composition Limits (in %)

Cu	Mg	Si	Fe	Mn	Zn	Ti	Cr	Other elements Each	Other elements Total
0,1	0,6 1,2	0,7 1,3	0,5	0,4 1,0	0,2	0,1	0,25	0,05	0,15

Outstanding Characteristics:

Medium strength alloy with good corrosion resistance.

Standard Commodities:

Plate; sheet; extrusions.

Typical Uses:

For stressed structural applications, such as bridges, cranes, roof trusses, transport applications. Beer barrels; milk churns. Bridle plates for man cages and ore skips.

Typical Physical Properties

Density	2,70	g/cm³
Modulus of Elasticity	70	GPa
Modulus of Rigidity	26,5	GPa
Melting Range	555–650	°C
Specific heat between 0–100 °C (273–373 K)	0,88	J/gK
Coefficient of linear expansion between 20–200 °C (293–473 K)	24×10^{-6}	/K
Thermal Conductivity at 100 °C (373 K)	180–189	W/mK
Resistivity at 20 °C (293 K)	$0{,}038 \times 10^{-8}$	Ω m

Other Characteristics

Corrosion Resistance	: Good
Weldability	: Good
Formability	: Good
Machinability	: Good
Anodizing	: Good
Brazeability	: Good

Mechanical Properties

Commodity and Temper	Gauge mm	0,2 % Proof Stress MPa	Ultimate Tensile Strength MPa	Elongation A_5 %	Brinell Hardness HB	Ultimate Shear Strength MPa
Sheet						
O	0,2–3,0	(60)	(125) 155	16 (30)	(32)	
T4	0,2–3,0	120 (200)	200 (250)	15 (18)	(70)	120 (155)
T6	0,2–3,0	255 (305)	295 (330)	8 (13)	(100)	175 (205)
Plate						
T4	up to 25	115 (185)	200 (230)	15 (22)	(60)	120 (160)
T6	up to 25	240 (280)	295 (325)	8 (10)	(95)	175 (205)
Extrusions						
O	up to 130		(170)	14		
F	up to 75		110	12		
T4	up to 75	120 (190)	190 (275)	14 (18)		
T6	up to 20	255 (315)	295 (330)	7 (10)		
T6	20–75	270 (320)	310 (345)	7 (12)		
T3	up to 6	115	215	12		
T3	6–10	115	215	14		
T8	up to 6	255	310	7		

Heat Treatment

Solution Heat Treatment				Ageing	
Temper	Temperature °C	Time h	Quenching	Temperature °C	Time h
T6	520 ± 3		In water	175 ± 3	10

Annealing

Temperature °C	Time h	
340–360	2	To soften partially.
340–360	2*	To soften fully.

*Cool not faster than 15 °C/hour to 250 °C and withdraw from furnace.

Appendix C:

Experiment 1: Relationship between metal deformation and e.m.f.
Aim: To see whether an e.m.f. will be generated merely by the deformation of the metal crystal structure
Action: The shaper was set up to confirm whether there is a significant e.m.f. change in the e.m.f. signal that is observed when the tool work-piece junction is stressed:

- The tool is brought into contact with the work-piece so that it gently touches
- The computer data sampling is started and the load on the tool is gradually increased by manually feeding the work-piece against the tool. By doing this the tool-work-piece junction is stressed and the metal at the junction is gradually deformed.
- The sampled data is then analysed after the experiment is complete by checking if the e.m.f. changed when the junction was loaded.

Experiment 2: Calibration of thermocouple
Aim: To obtain data to calibrate the tool/workpiece thermocouple. This gives an indication of the temperatures that are attained when the aluminium is being cut.
The temperature is measured by using the dissimilar metal junction formed by the tool and the workpiece as a thermocouple. The e.m.f. that is generated at this junction is an indication of the temperature at the junction, i.e. the temperature is a function of the e.m.f.
Action:

- The workpiece is cast in light weight concrete
- The cast with the workpiece in it is clamped in the chuck on the shaper.
- A hole is drilled at both ends of the workpiece
- The tool is manually fed into the workpiece
- An RTD (resistance temperature device) is inserted in the hole closest to the point where the tool/workpiece junction is and an aluminium lead into the other. The RTD was very close to the junction i.e. 5mm.
- The cold junctions are kept at 23°C.
- The data sampling program on the computer is started and the workpiece is heated gradually with a blow torch.
- The computer writes both the RTD measured temperature and the e.m.f. that is generated at the junction on a file for later use for tool/workpiece thermocouple calibration.
- The blow torch is never closer than 40mm to the junction and the RTD.
- When the workpiece starts to melt heating is stopped and the workpiece is left to cool down.
- Plot the e.m.f. vs. temperature data and obtain the appropriate polynomial by regression by which the two variables are related.

Experiment 3: Calibration of strain gauge
Aim: To obtain data to calibrate the strain gauge.
Action:

- Clamp the tool on a robust flat metal surface so that the distance between the cutting edge and the last point of support of the tool is the same as it will be when cutting metal on the shaper.
- Tune the trimpot on the strain amplifier/signal amplifier so that the output is 0.000V for 0N load.
- Use a specially adapted hanger of known mass and hang it on the tool tip.
- Measure the voltage after it has been amplified by the signal amplifier and write down the load on the tool and the corresponding voltage.
- Repeat increasing the load and writing down the load and the corresponding voltage until five data points have been accumulated.
- The relationship between the load and the voltages observed is linear. Do linear regression and find it.
- Use the mathematical relationships determined in experiments 2 and 3 in the computer program to output the temperature and cutting force data directly to screen and to file.

Experiment 4: Cut characterisation
Aim: To obtain cutting force and temperature data for cutting metal when various cutting fluids are used.
Action:

- Mark the workpiece at the quarter-, half- and three quarter- way mark with permanent marking ink of different colours.
- Know the length of the cut that will be made and the rake face angle.
- Remember to check the reference points
- Keep all cutting parameters constant
- Use bi-directional restraint of chip flow, i.e. choose a feed on the shaper such that the material flow during chip formation is restrained from both sides and so that no cut will overlap with a previous cut.
- Change only the type of cutting fluid used in each experiment
- Make sure that the cutting fluid applicator applies cutting fluid to the tool before the tool is engaged into the workpiece.
- Make sure that the cutting fluid used is the cutting fluid used and does not have residual cutting fluid or cleaning solvent from the previous test in it. This may be ensured by letting the applicator spray for a while after changing cutting fluids.
- Make sure that the tool is clean, i.e. that it has no residual metal left on it or cutting fluid from a previous test.
- Set the tool on the shaper so that it has some time to travel freely before it starts cutting the metal.
- Activate the computer program for data sampling
- Switch on the lubricant applicator if cutting fluid is used.
- Switch on the shaper and once the cut is complete switch it and the lubricant applicator off again.

- Perform the dry cuts first. Then do the cuts for the different cutting fluids. Ten per cutting fluid should suffice.
- Do one cut at a time so that the chip can be collected without confusion between chips from different cuts.
- Store each chip with a reference to the file on which the cut data appears.
- Check that the chip masses are more or less the same, say 200mg. This way it is ensured that the depth of cut is constant.
- Plot the cutting force and temperature data from the tests and check for repeatability
- Next measure the length of the first quarter of the chip. The ratio of the original one quarter length to this quarter length is the mean chip thickness ratio
- Calculate and tabulate the shear plane angle and the chip strain
- Photograph the chips as a group for the different cutting fluids used.
- Visually inspect the underside of the chips and note the smooth fraction of the chip i.e. where no marked scratching or dulling of the underside surface appears.
- Do this for each chip series in each cutting fluid
- Calculate the average smooth fraction from this for each cutting fluid
- Tabulate the data
- Similarly as for the smooth fraction determine the average fraction to first break for the chips and compute the average distance to first break from this.
- Tabulate the data
- Choose a representative chip from each group and make SEM micrographs
- Observe and tabulate the deformation / flow-zone thickness
- Choose a chip from each group and mount it in thermoset resin
- Sand the mount down until the longitudinal lateral mid cross-section of the chip is exposed and polish this section to a high fineness.
- View the cross section under an optical microscope
- If nothing is observed in terms of metal deformation etch the chip with 0,5% HF in distilled water for 30 seconds
- Immediately after that flush the chip with alcohol and blow it dry
- View it again under the optical microscope and if still nothing is seen etch again for ten seconds
- Repeat the previous step until the metal deformation becomes clear.
- Make micrographs of the metal deformation in the chip.
- Compare the deformation with that observed on the SEM micrographs.
- Make micro-hardness measurements on the mounted chips close to the one quarter mark and set up chip hardness profiles for each mounted chip.
- Plot the hardness profiles and tabulate the flow-zone thickness that may be determined from these profiles and compare this to the results obtained from the micrographs
- Tabulate the average chip hardness, as calculated from the last three hardness measurements furthest away from the flow-zone.
- Compare all the accumulated data for all the cutting fluids.

Experiment 5: Surface roughness determination
Aim: To obtain surface roughness data for the different cutting fluids that were used.
Action:

- Be sure that the cutting fluid that is to be used is uncontaminated
- Make sure the tool is clean
- Use a fine feed
- Switch on the cutting fluid applicator and the shaper
- Perform metal cutting until a 15 mm width has been cut off the surface of the workpiece
- Mark this width on the work piece
- Bleed the cutting fluid applicator and change the cutting fluid and repeat the above exercise for each cutting fluid that is to be tested.
- Use a profilometer and determine the surface roughness at the beginning middle and end of each surface produced for the different cutting fluids that were used.
- Do these surface roughness measurements longitudinally and transversely
- When doing the longitudinal measurements be careful not to cross over ridges on the machined surface. These ridges can be avoided by taking many measurements. The lowest of these can be taken as measurements where no ridge was crossed.
- Tabulate the data and compare it for the different cutting fluids that were used.

Experiment 6: Micrographic observation and micro-hardness determination
It is suspected that the BUE phenomenon is present and therefore a lateral cross-section of the tool chip interface should be made. This should be etched with an appropriate solution such as hydrofluoric acid until the metal deformation can be seen clearly when it is examined under the optical microscope. This cross-section could also be examined under the scanning electron microscope (SEM). Micro-hardness tests should also be done on this chip to see what the effect of the built-up edge is on the hardness profile of the chip.

A non-etched chip sample can be analysed by SEM and/or MS for type of atoms that are present on the underside of the chip surface and in the chip after cutting when good cutting results are obtained. For an analysis in the chip a longitudinal cross section should be used.

Likewise examining the tool cutting edge and rake face by SEM, or mass ion spectroscopy (MIS) could give an indication of which atoms are present. This could give an indication of which atoms are desired when this examination occurs after pleasing results from a mechanical parameter investigation are obtained. If more detail is required FTIR (Fourier transform infrared) spectroscopy can be used for identification of the metal compounds that do form.

Experiment 7: Effect of cutting speed on built-up edge
Aim: To see whether the built-up edge forms later, i.e. at a greater length of cut when the cutting speed is increased and to see the effect of this on the cutting temperature and the cutting forces.
Action:
- Perform cuts and increase the cutting speed for each cut that is made
- Keep all other parameters constant
- Present the results graphically

Results and Discussion of Experiments for Preparation of Equipment

The main results for the cutting process investigation were presented in chapter 8 and are the results of experiments 4 -7.

As regards experiment 1 that was used to show the effect of stressing the tool on the e.m.f. that is generated it was found that the e.m.f. is unaffected. The tool was gradually statically loaded and no change in the e.m.f. was seen.

In experiment 2 that was done to calibrate the tool workpiece thermocouple the following was found: (see figure C.1). The lower of the two curves in figure C.1(b) is the same as the curve in figure C.1(a). The hysteresis that resulted is interesting. It is due to the temperature sensor being imbedded in the aluminium workpiece cooling at a slightly slower rate than the tool/workpiece junction that is situated on the surface of the workpiece. The actual temperature of the top curve should thus have been lower and the top curve would have been very much closer to the bottom curve.

Curve fitting on the data points resulted in a fourth order polynomial of very good fit over the temperature range 30°C to 523°C, i.e. 0.4 to 2.0V. The regression coefficient was 0.9903. For temperatures above 520°C the slope of the line between 1.5V and 1.9V was used to extrapolate the temperature for the measured e.m.f.
The alloy melts at 565±5°C as measured by the RTD.
In experiment 3 the relationship (eqn. C.1) between the cutting force and the microvolt signal was found as:

$$Cutting\ \ Force = 232.2/1000000 \cdot X \qquad \text{Eqn.C.1}$$

Where X is the microvolt signal.
For the method used see Appendix C, experiment 3.

Both the results of experiments 2 and 3 were applied to get results in experiment 4 and satisfactory results were obtained as is evident from the results presented for experiment 4. (See chapter 8)

a)

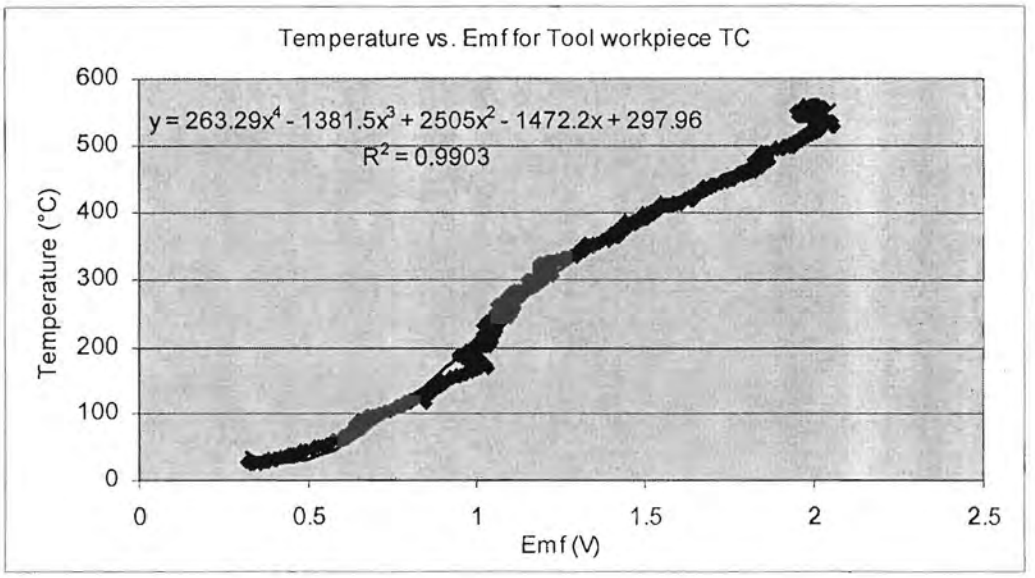

b)

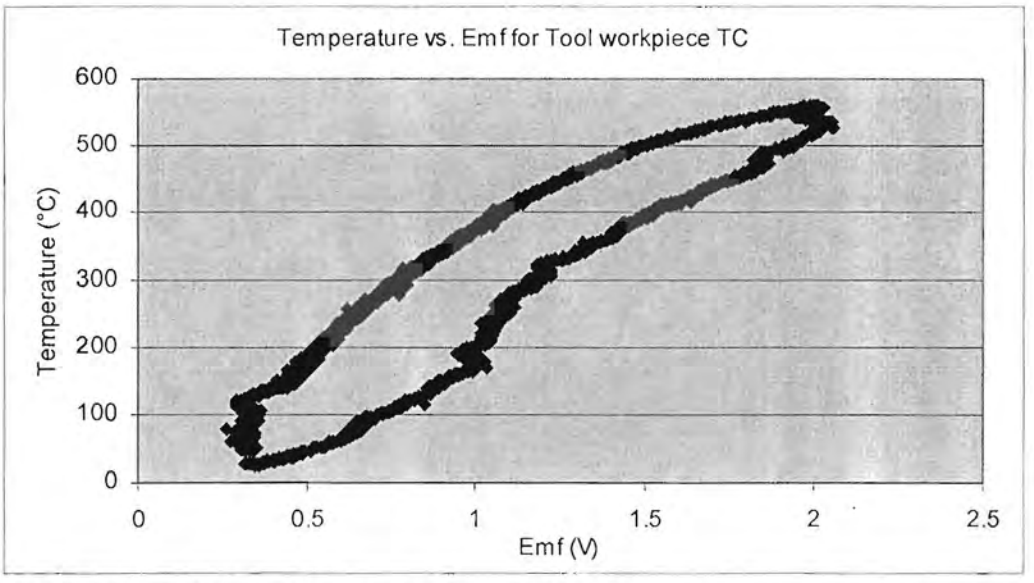

Figure C.1 Tool/workpiece thermocouple e.m.f. vs. Temperature response.

Cutting Force and Temperature: raw data	Cutting Force 5 point moving average : Sample and Dry	Cutting Temperature : Sample and Dry
C. force and Temperature for Test 1 of Carbon Tetra chloride 197mg	Compare C.forces CCl_4 T1 197 vs. DRY3 197 mg	Compare Temperature CCl_4 T1 197 vs DRY3 197 mg
CCl_4 T2 C. force and Temperature 197 mg	Compare C.forces CCl_4 T2 197 vs DRY3 197 mg	Compare Temperature CCl_4 T2 197 vs DRY3 197 mg
CCl_4 T3 C. force and Temperature 197 mg	Compare C.forces CCl_4 T3 197 vs DRY3 197 mg	Compare Temperature CCl_4 T3 197 vs DRY3 197 mg

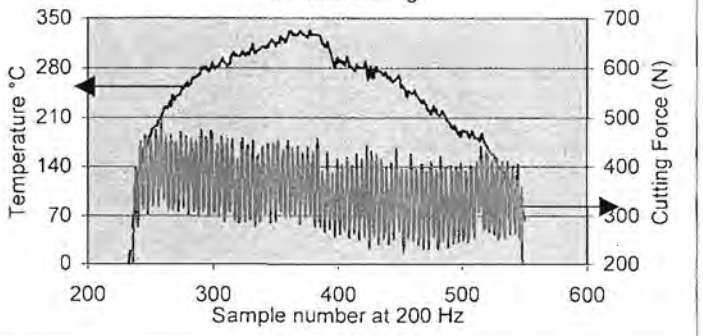

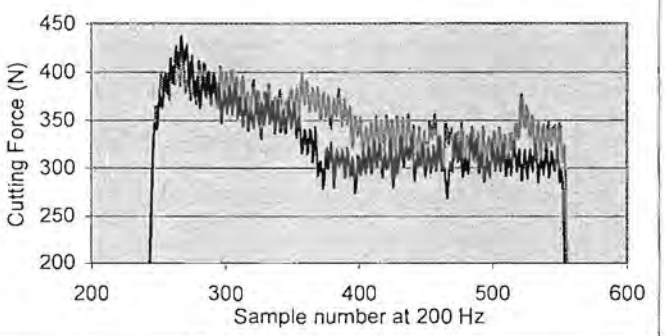

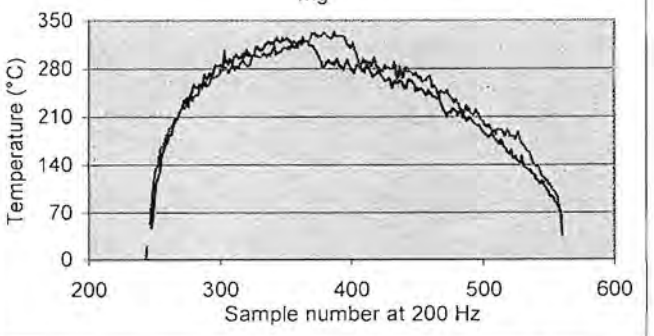

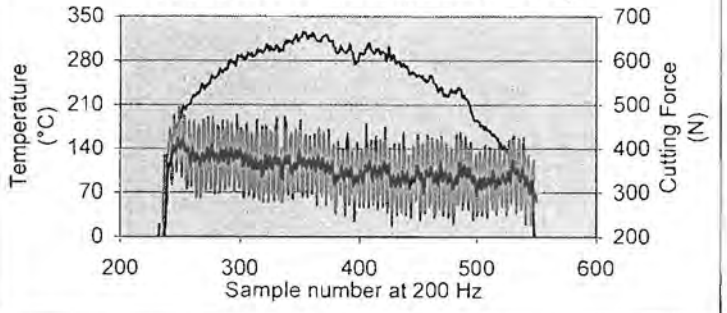

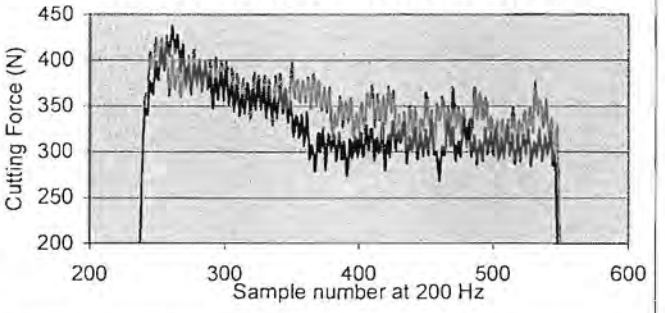

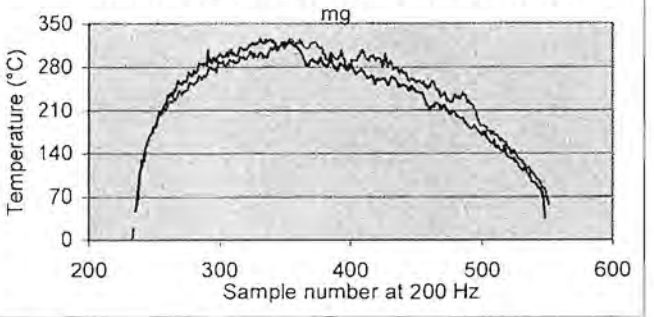

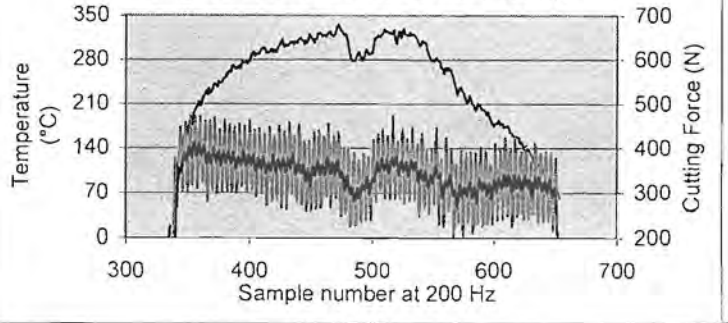

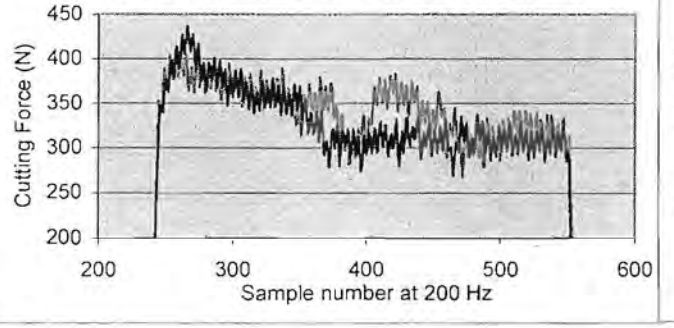

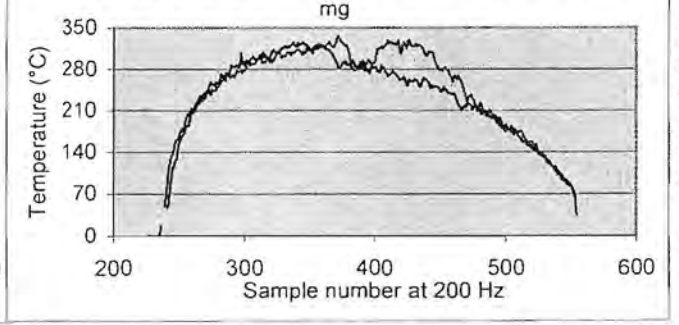

Appendix D

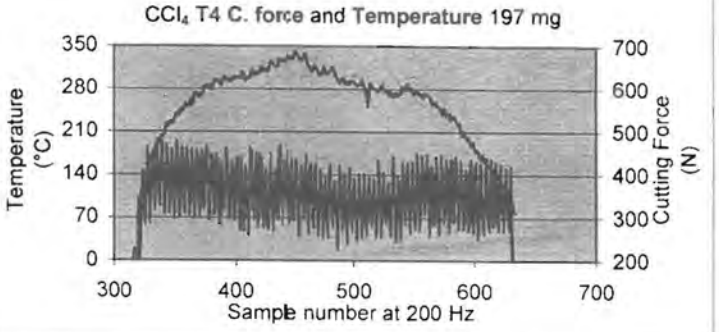
CCl4 T4 C. force and Temperature 197 mg
Temperature (°C)
Cutting Force (N)
Sample number at 200 Hz

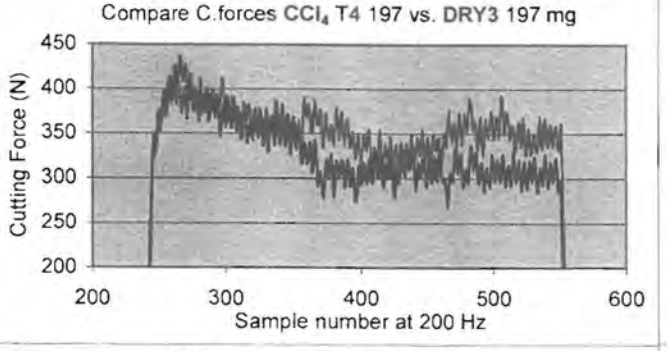
Compare C.forces CCl4 T4 197 vs. DRY3 197 mg
Cutting Force (N)
Sample number at 200 Hz

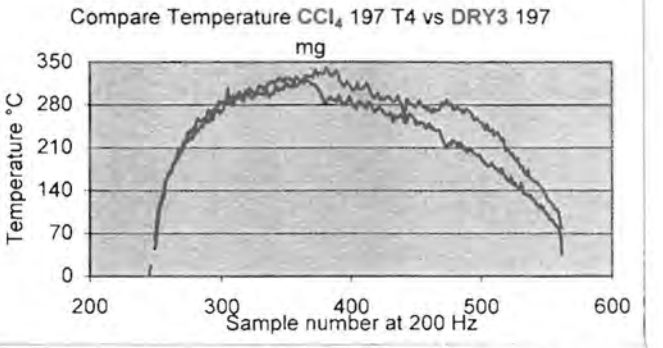
Compare Temperature CCl4 197 T4 vs DRY3 197 mg
Temperature °C
Sample number at 200 Hz

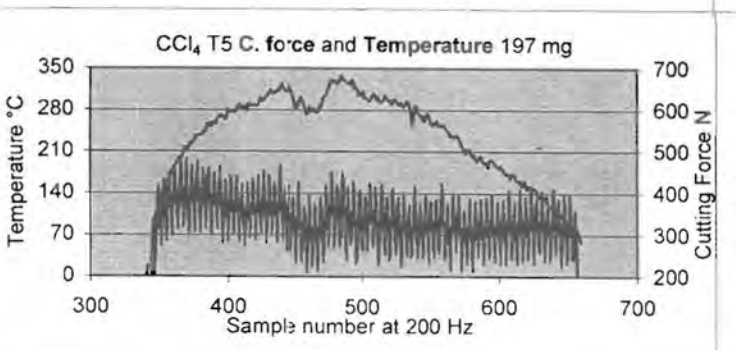
CCl4 T5 C. force and Temperature 197 mg
Temperature °C
Cutting Force N
Sample number at 200 Hz

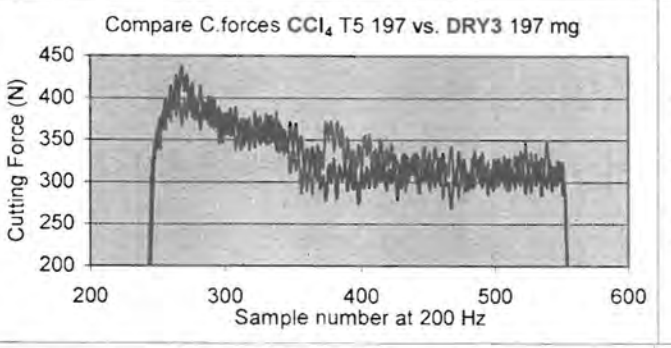
Compare C.forces CCl4 T5 197 vs. DRY3 197 mg
Cutting Force (N)
Sample number at 200 Hz

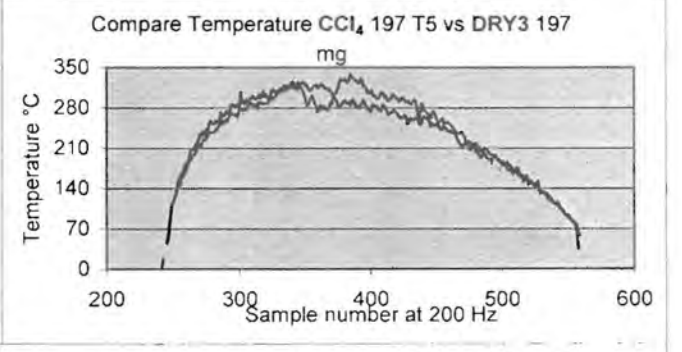
Compare Temperature CCl4 197 T5 vs DRY3 197 mg
Temperature °C
Sample number at 200 Hz

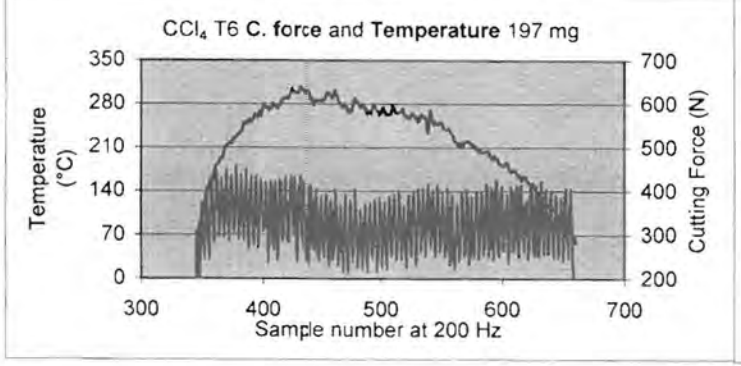
CCl4 T6 C. force and Temperature 197 mg
Temperature (°C)
Cutting Force (N)
Sample number at 200 Hz

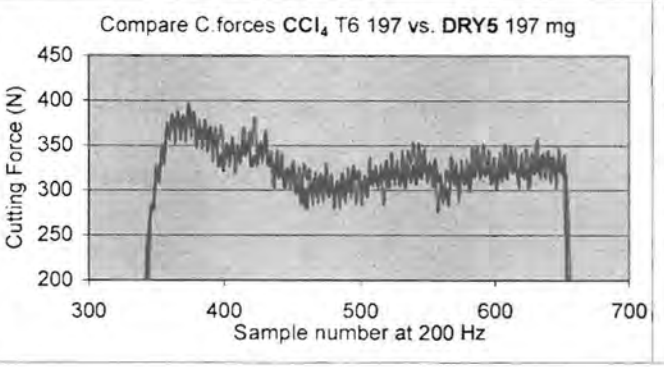
Compare C.forces CCl4 T6 197 vs. DRY5 197 mg
Cutting Force (N)
Sample number at 200 Hz

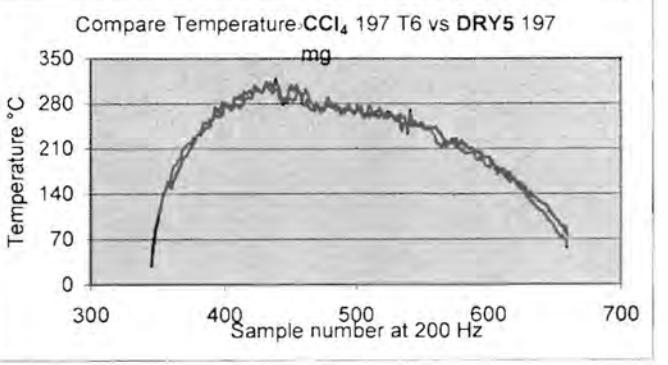
Compare Temperature CCl4 197 T6 vs DRY5 197 mg
Temperature °C
Sample number at 200 Hz

Cutting Force and Temperature: raw data	Cutting Force 5 point moving average : Sample and Dry	Cutting Temperature : Sample and Dry
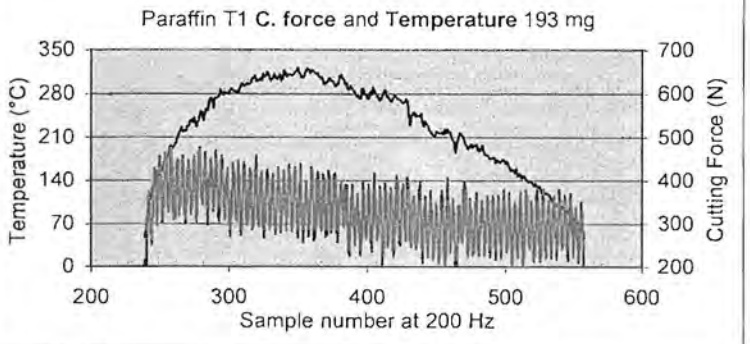	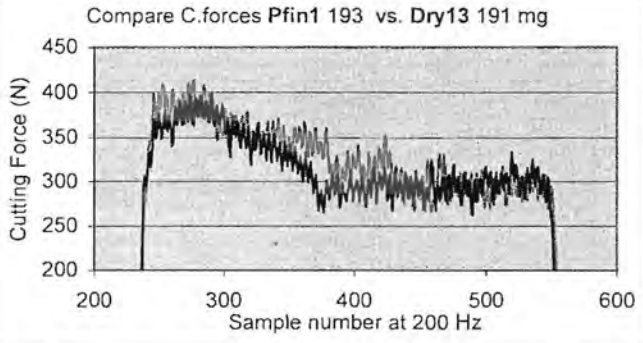	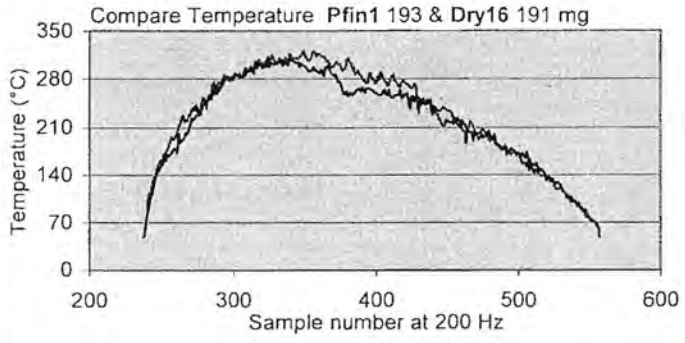
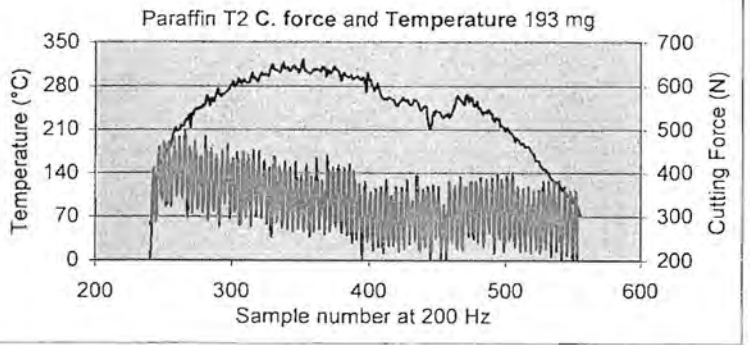	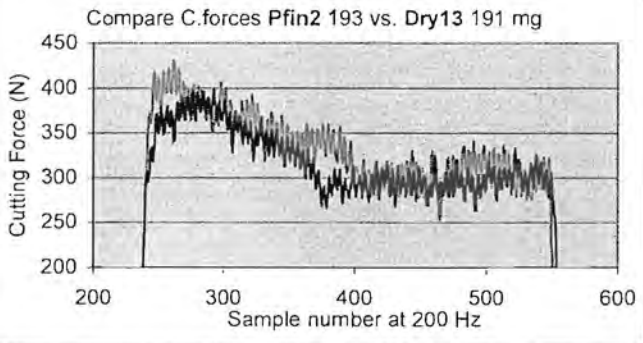	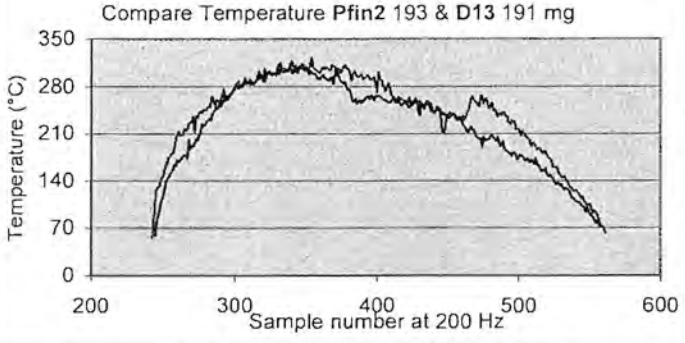
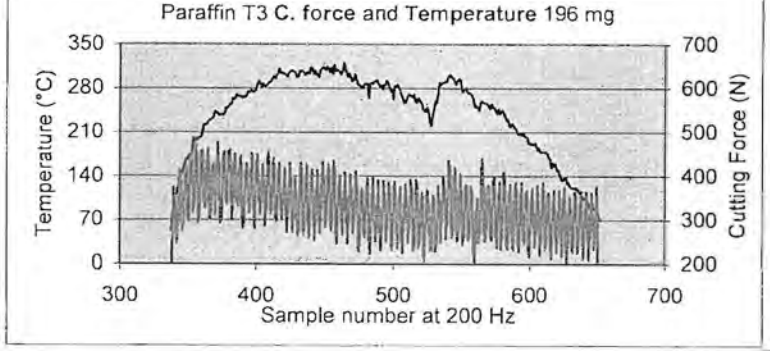	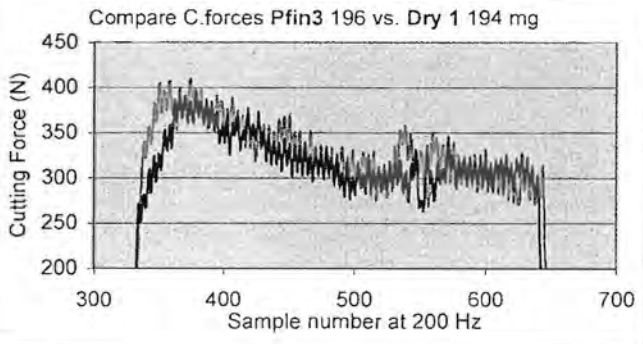	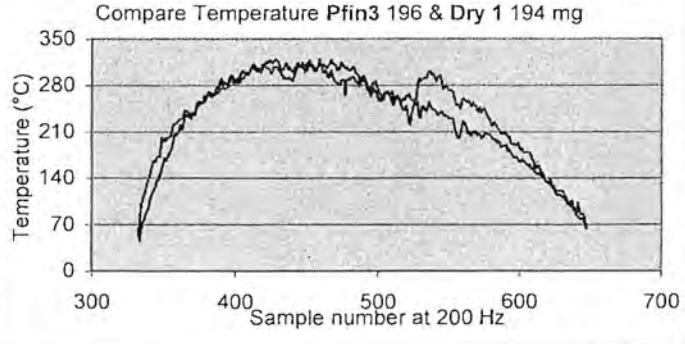

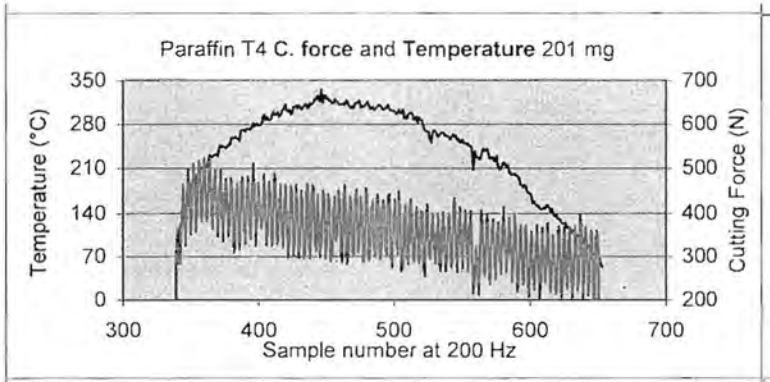
Paraffin T4 C. force and Temperature 201 mg
Temperature (°C)
Cutting Force (N)
Sample number at 200 Hz

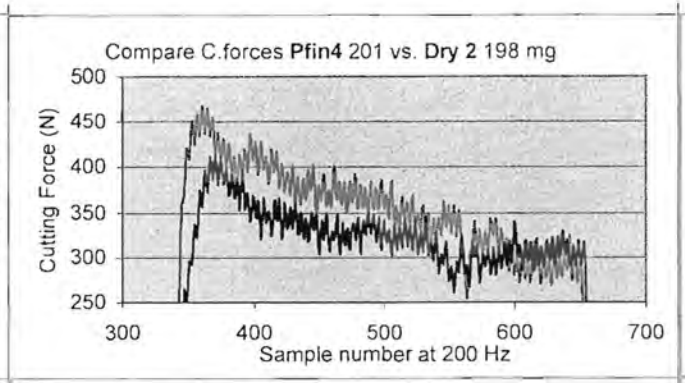
Compare C.forces Pfin4 201 vs. Dry 2 198 mg
Cutting Force (N)
Sample number at 200 Hz

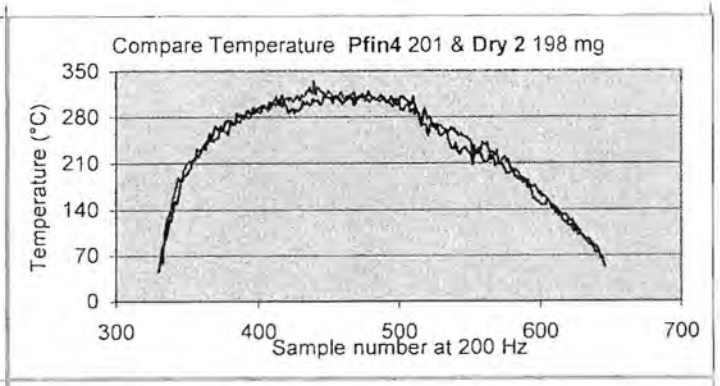
Compare Temperature Pfin4 201 & Dry 2 198 mg
Temperature (°C)
Sample number at 200 Hz

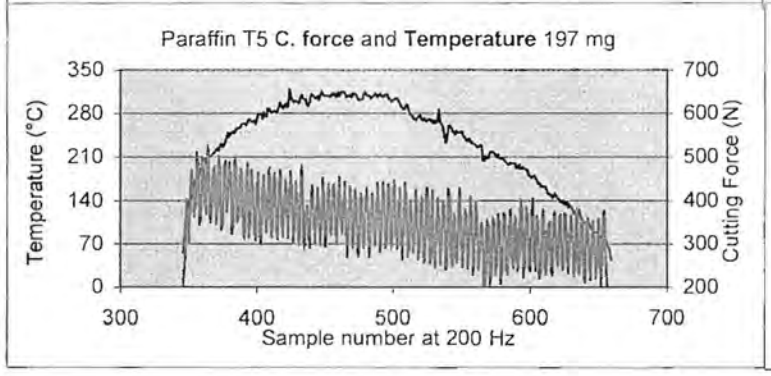
Paraffin T5 C. force and Temperature 197 mg
Temperature (°C)
Cutting Force (N)
Sample number at 200 Hz

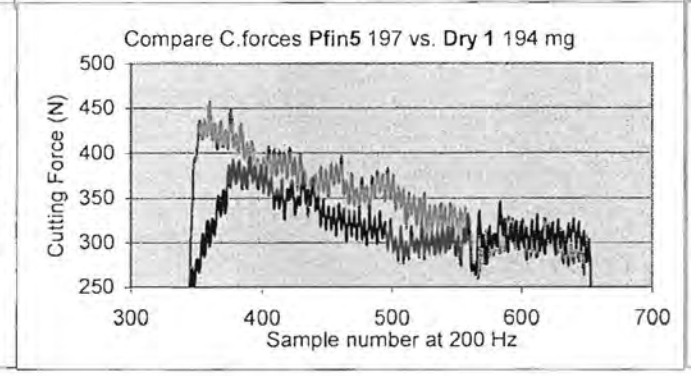
Compare C.forces Pfin5 197 vs. Dry 1 194 mg
Cutting Force (N)
Sample number at 200 Hz

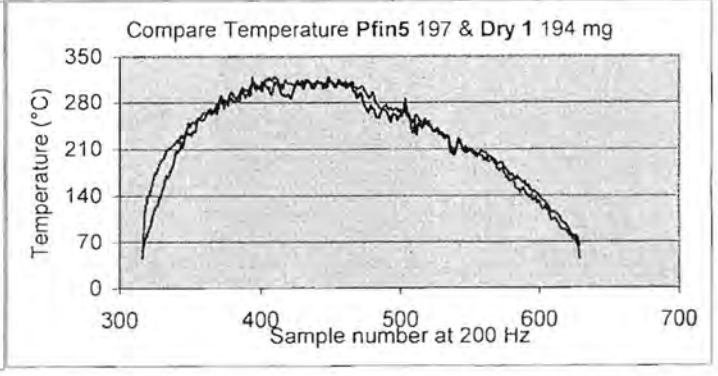
Compare Temperature Pfin5 197 & Dry 1 194 mg
Temperature (°C)
Sample number at 200 Hz

Cutting Force and Temperature: raw data	Cutting Force 5 point moving average : Sample and Dry	Cutting Temperature : Sample and Dry
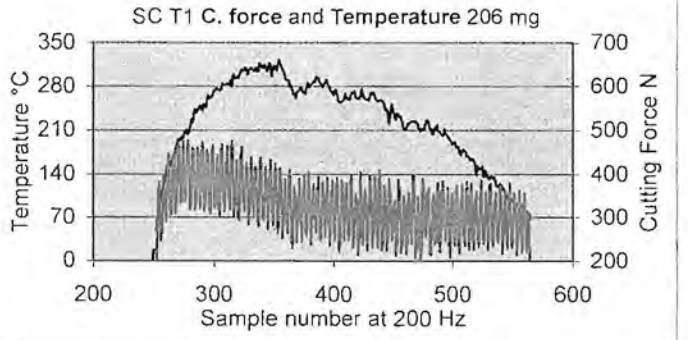	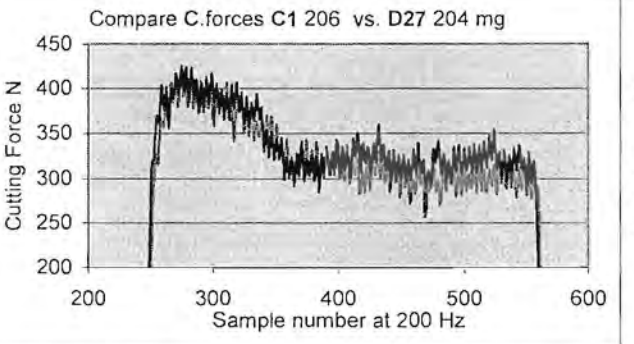	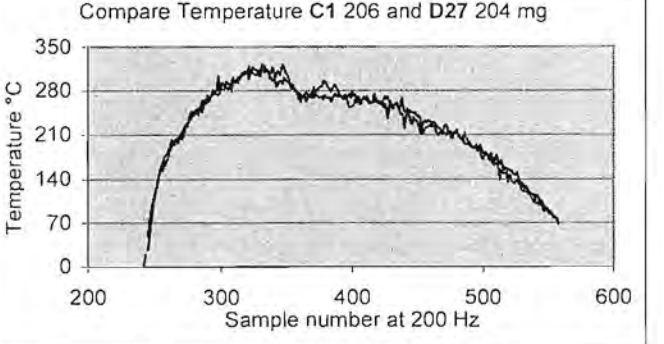
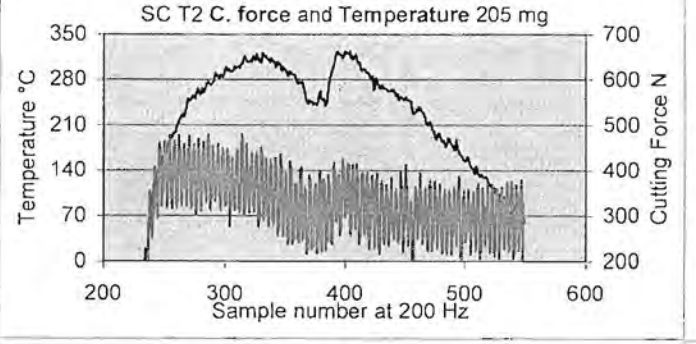	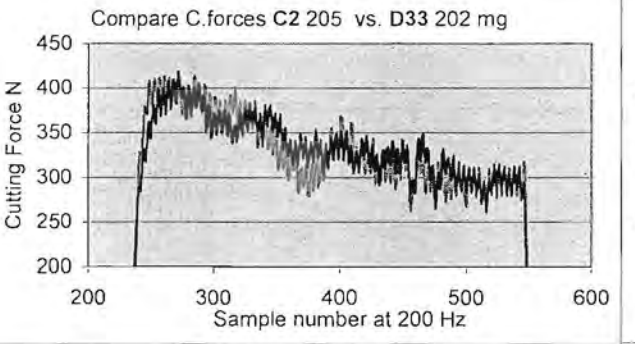	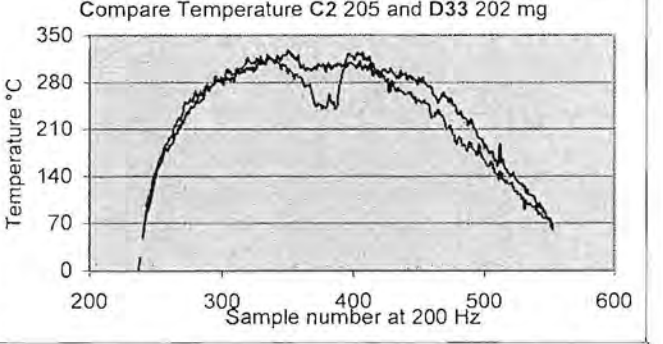
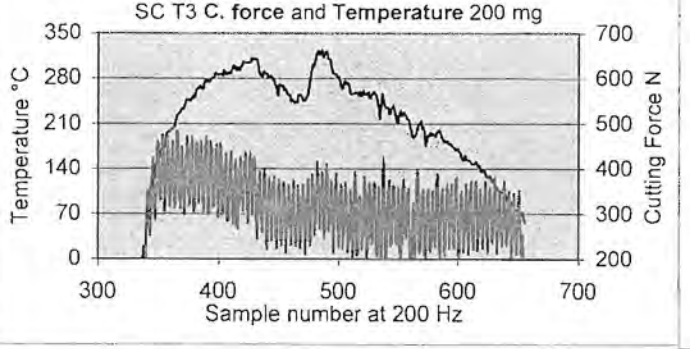	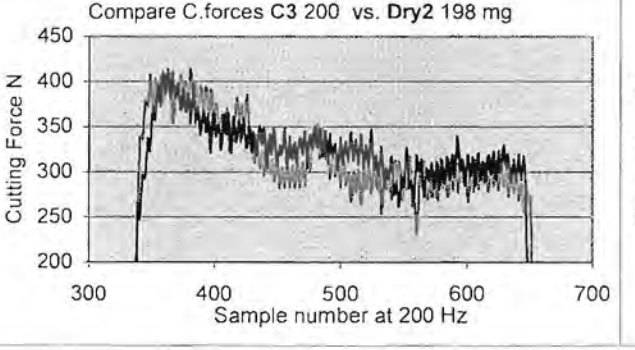	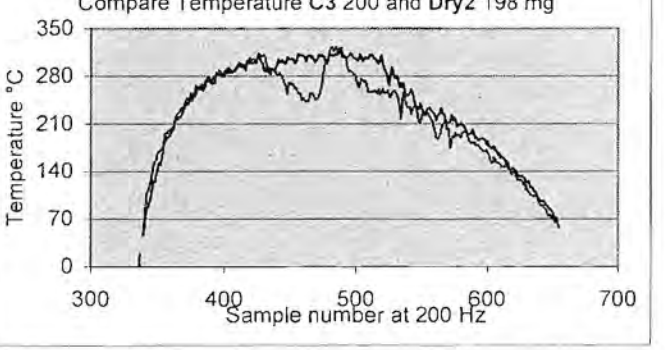

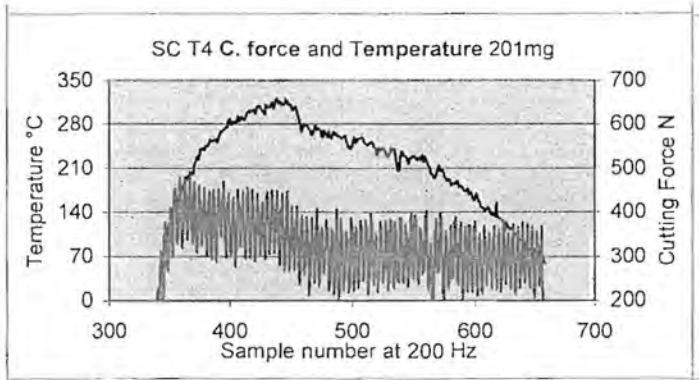
SC T4 C. force and Temperature 201mg
Temperature °C
Cutting Force N
Sample number at 200 Hz

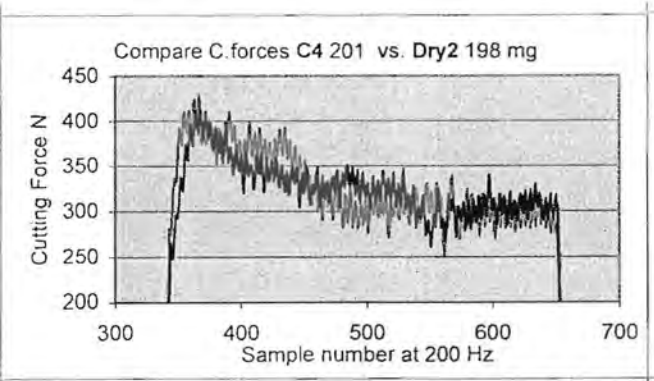
Compare C.forces C4 201 vs. Dry2 198 mg
Cutting Force N
Sample number at 200 Hz

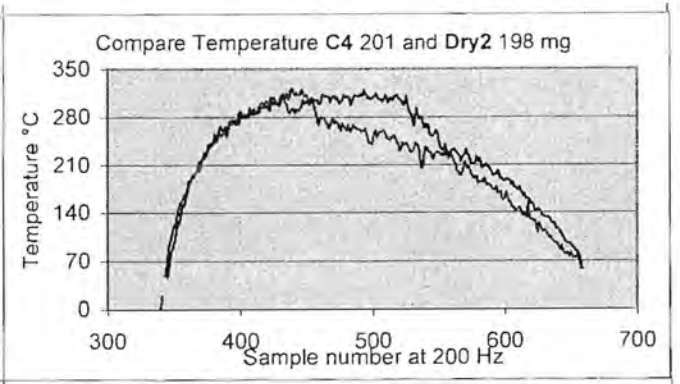
Compare Temperature C4 201 and Dry2 198 mg
Temperature °C
Sample number at 200 Hz

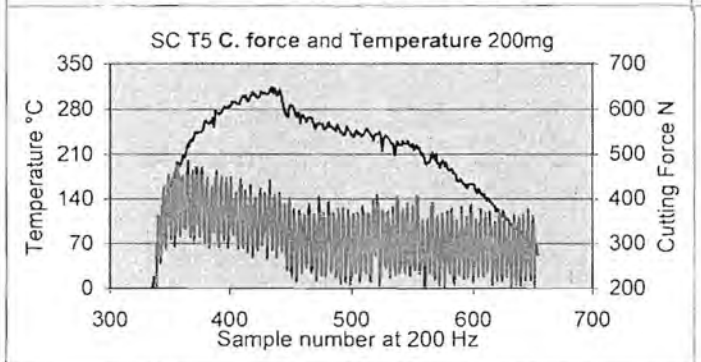
SC T5 C. force and Temperature 200mg
Temperature °C
Cutting Force N
Sample number at 200 Hz

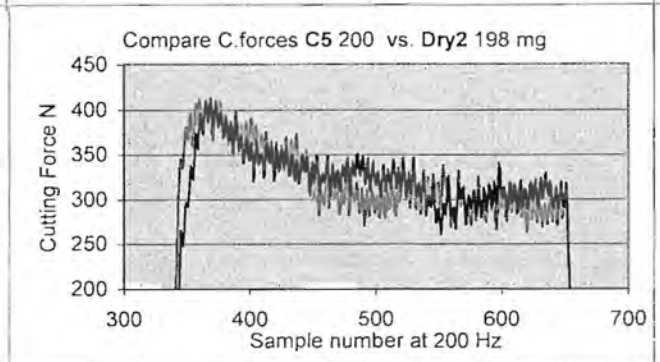
Compare C.forces C5 200 vs. Dry2 198 mg
Cutting Force N
Sample number at 200 Hz

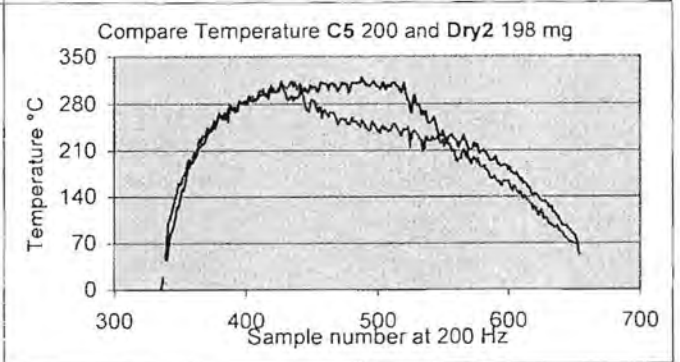
Compare Temperature C5 200 and Dry2 198 mg
Temperature °C
Sample number at 200 Hz

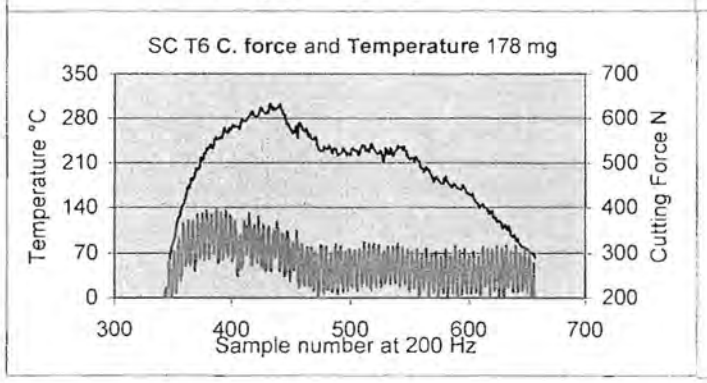
SC T6 C. force and Temperature 178 mg
Temperature °C
Cutting Force N
Sample number at 200 Hz

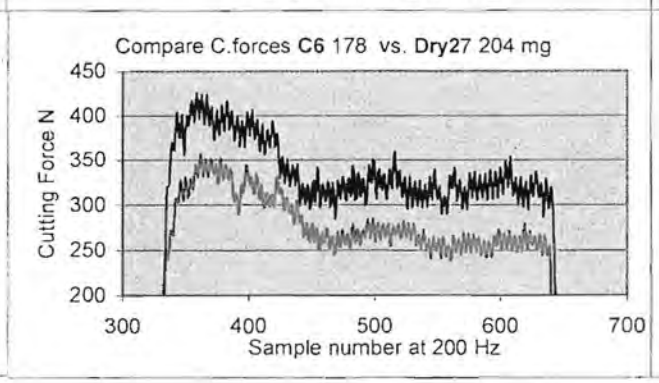
Compare C.forces C6 178 vs. Dry27 204 mg
Cutting Force N
Sample number at 200 Hz

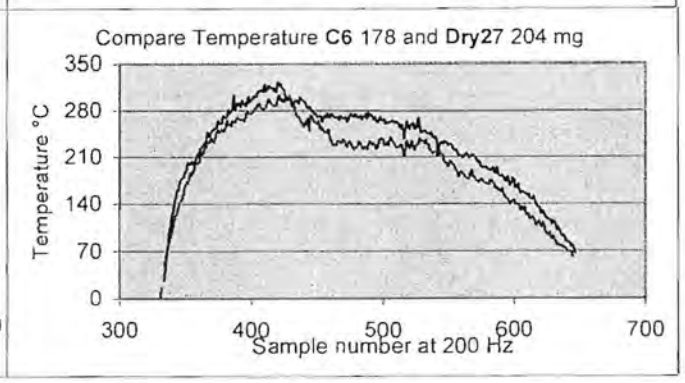
Compare Temperature C6 178 and Dry27 204 mg
Temperature °C
Sample number at 200 Hz

Cutting Force and Temperature: raw data	Cutting Force 3 point moving average : Sample and Dry	Cutting Temperature : Sample and Dry

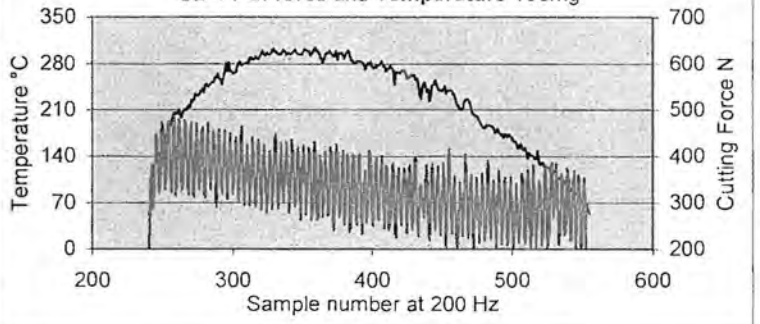

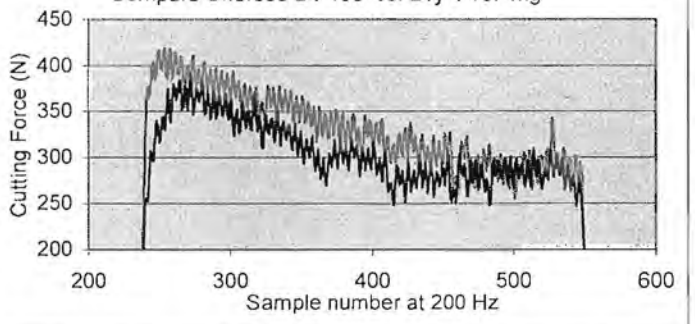

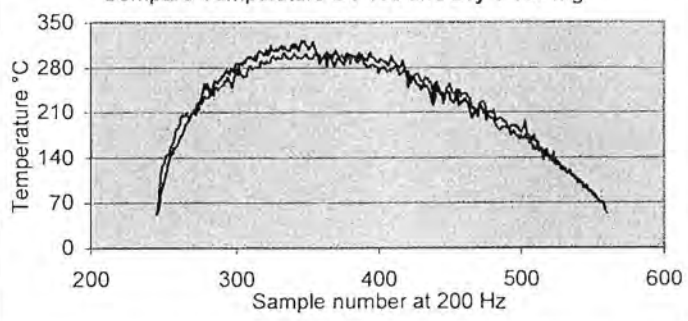

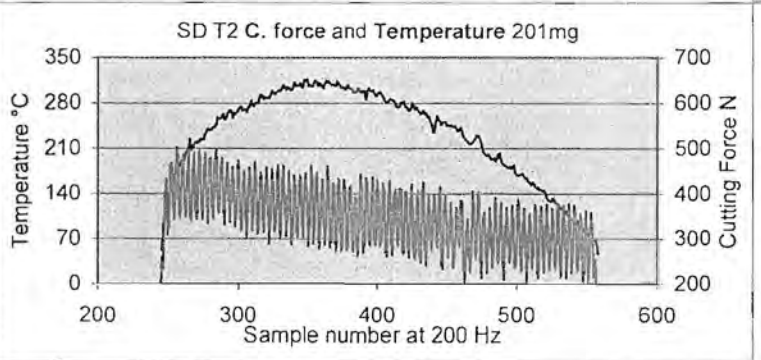

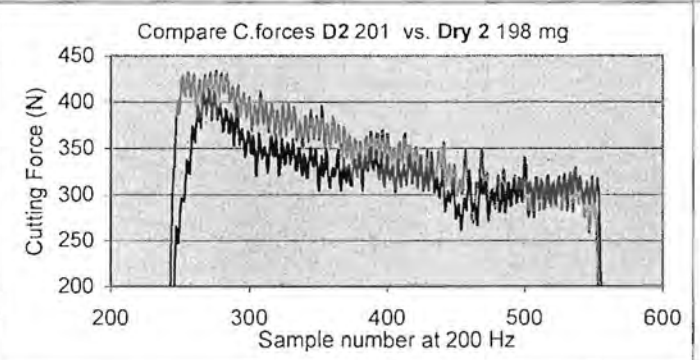

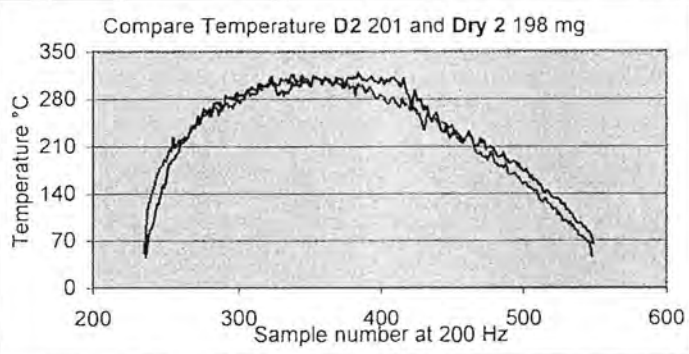

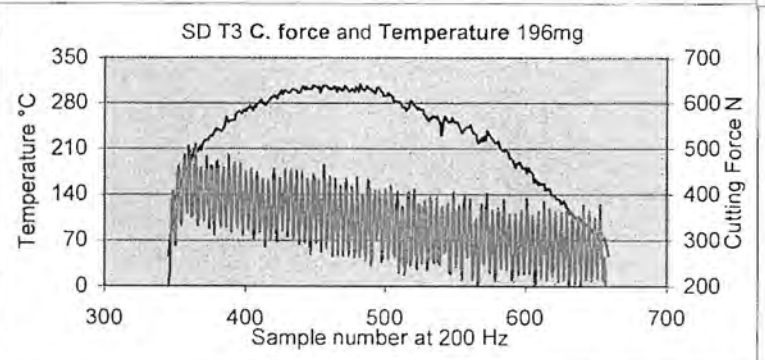

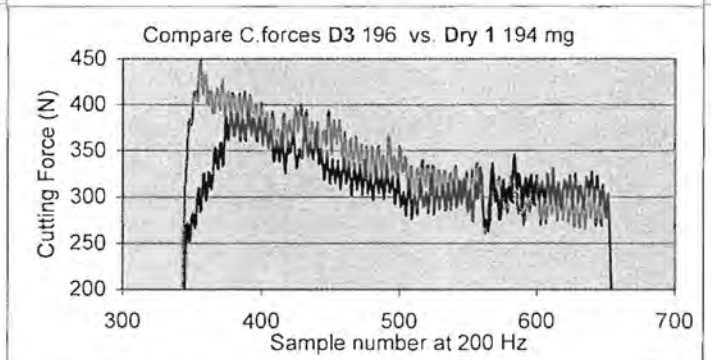

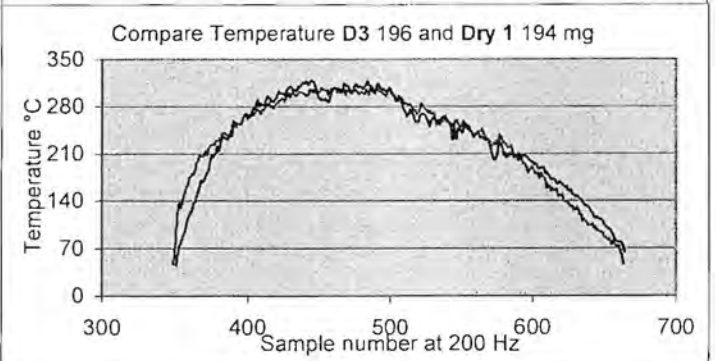

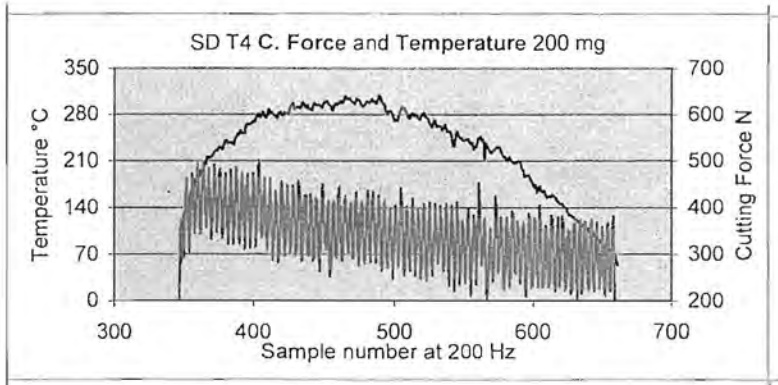

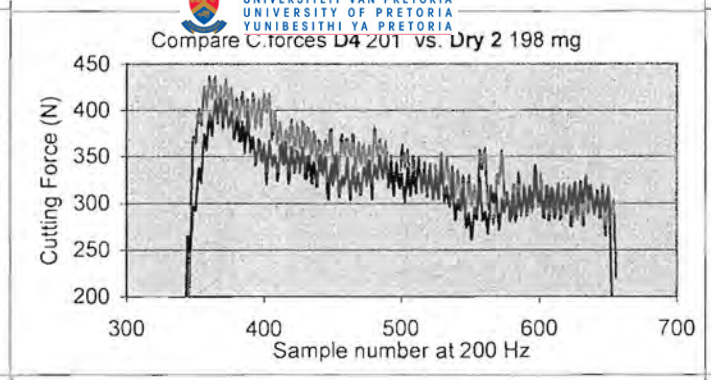

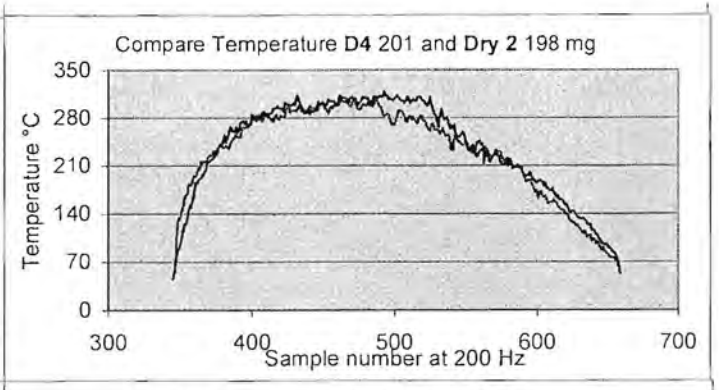

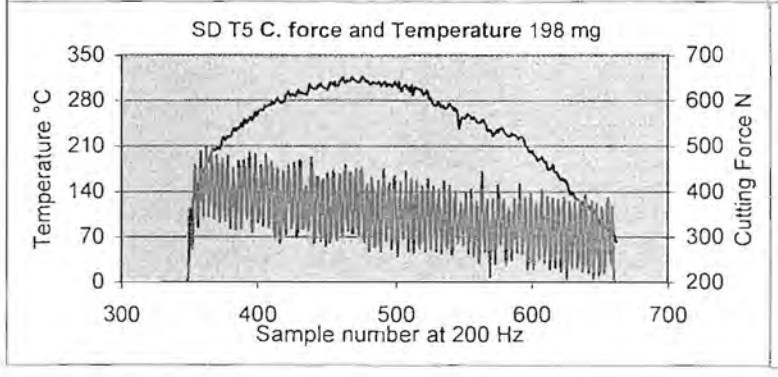

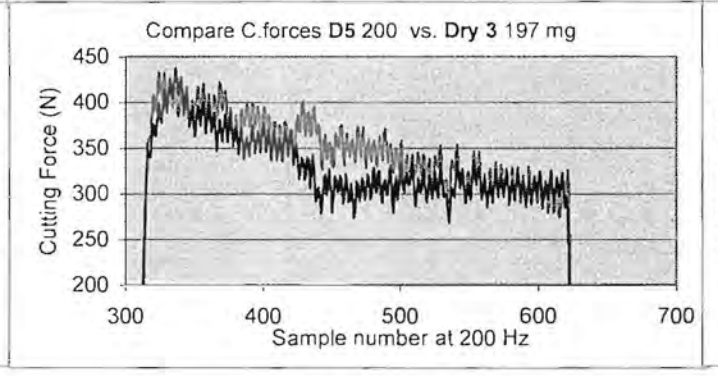

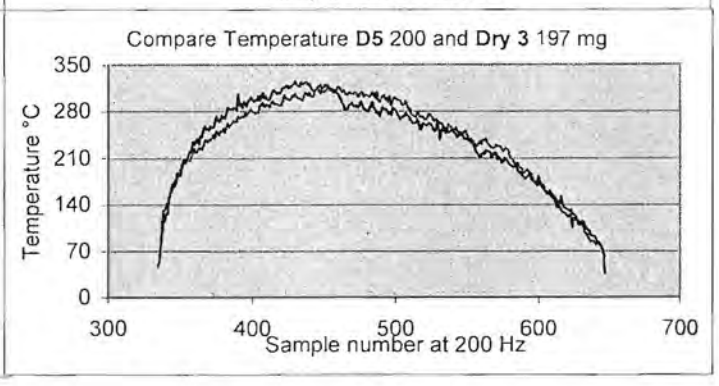

Cutting Force and Temperature: raw data	Cutting Force 5 point moving average : Sample and Dry	Cutting Temperature : Sample and Dry

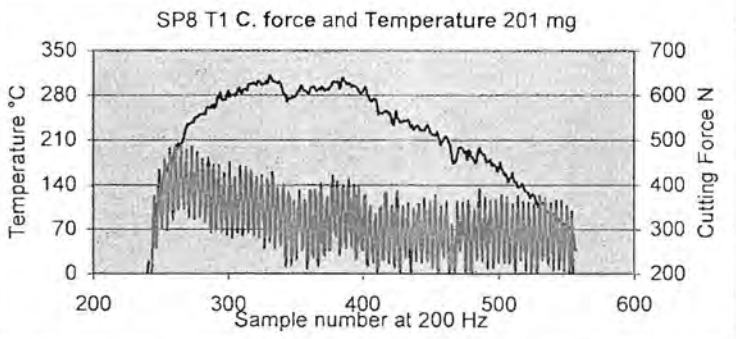

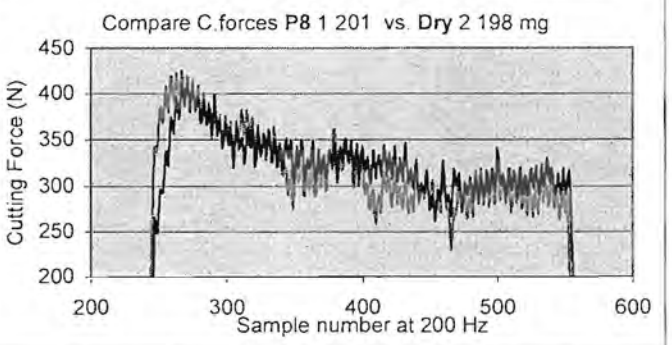

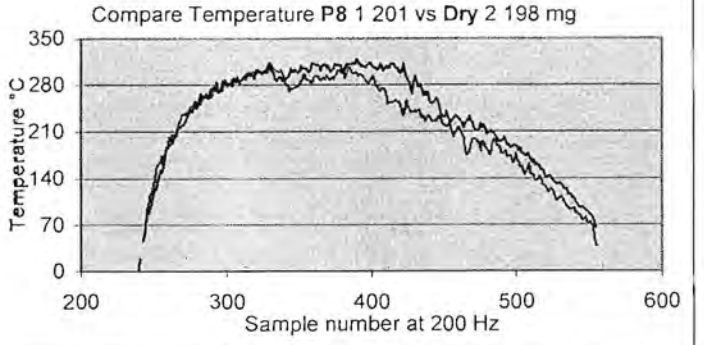

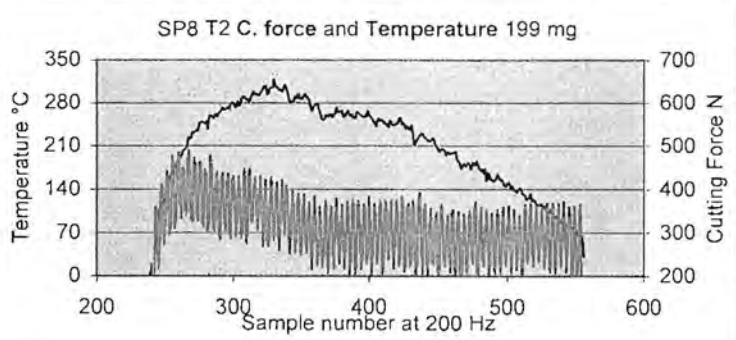

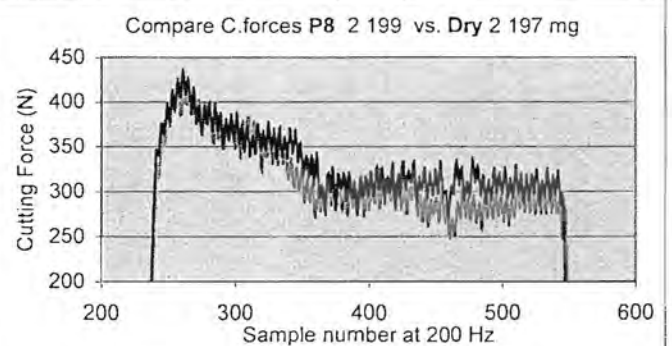

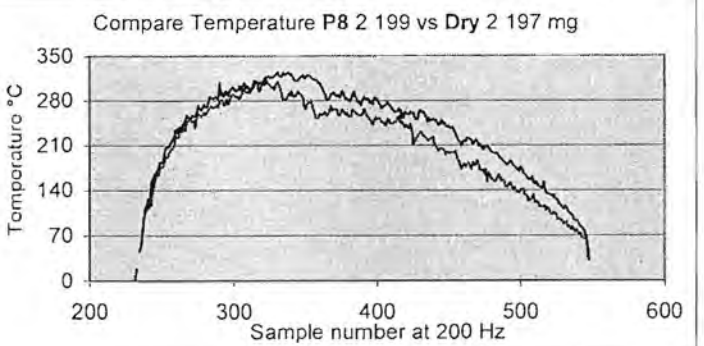

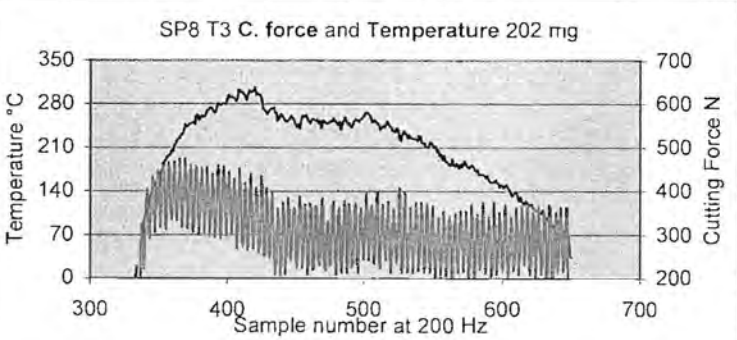

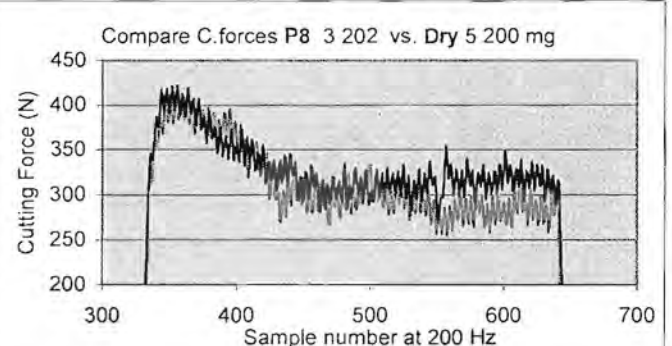

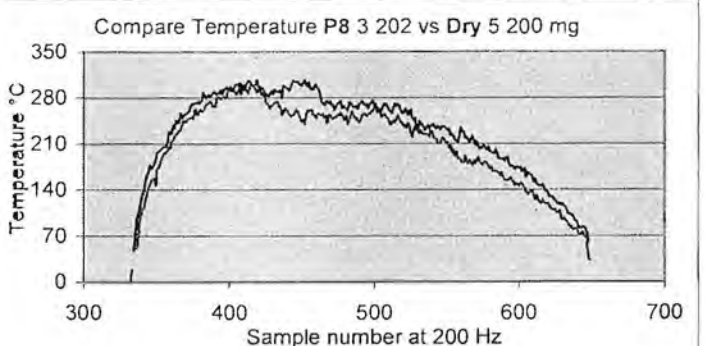

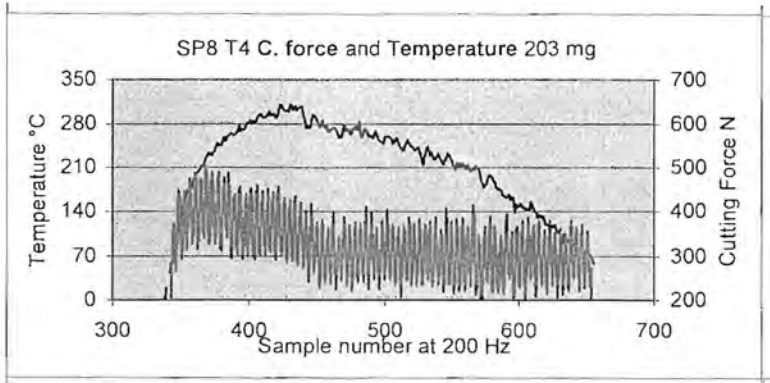
SP8 T4 C. force and Temperature 203 mg
Temperature °C
Cutting Force N
Sample number at 200 Hz

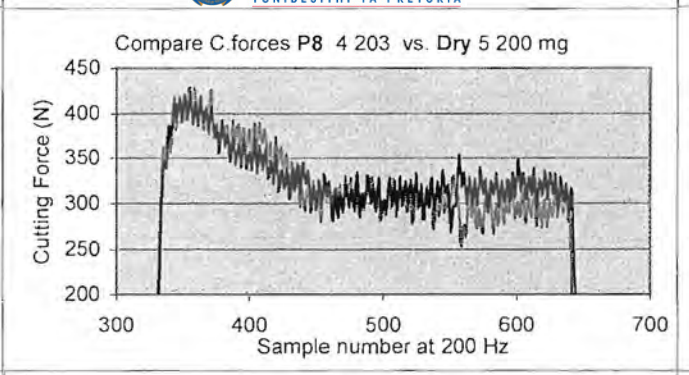
Compare C.forces P8 4 203 vs. Dry 5 200 mg
Cutting Force (N)
Sample number at 200 Hz

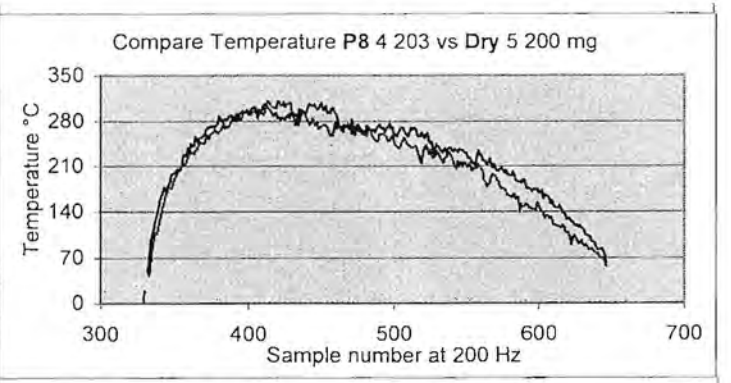
Compare Temperature P8 4 203 vs Dry 5 200 mg
Temperature °C
Sample number at 200 Hz

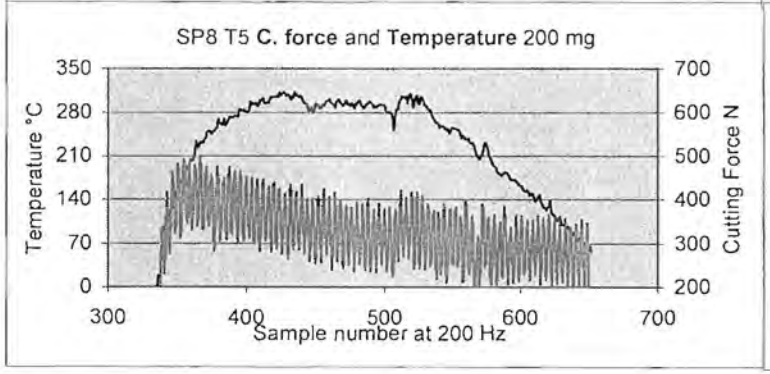
SP8 T5 C. force and Temperature 200 mg
Temperature °C
Cutting Force N
Sample number at 200 Hz

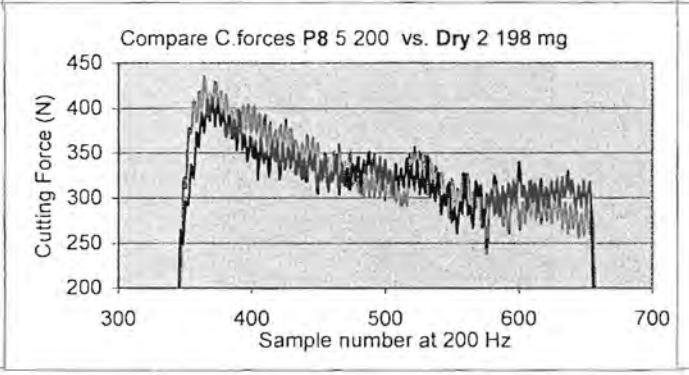
Compare C.forces P8 5 200 vs. Dry 2 198 mg
Cutting Force (N)
Sample number at 200 Hz

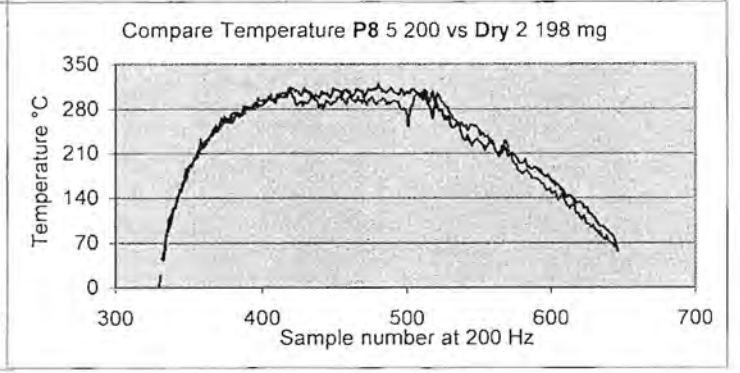
Compare Temperature P8 5 200 vs Dry 2 198 mg
Temperature °C
Sample number at 200 Hz

Cutting Force and Temperature: raw data	Cutting Force 5 point moving average : Sample and Dry	Cutting Temperature : Sample and Dry

20

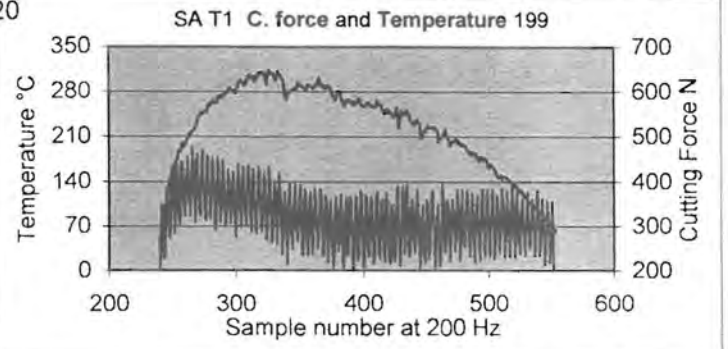

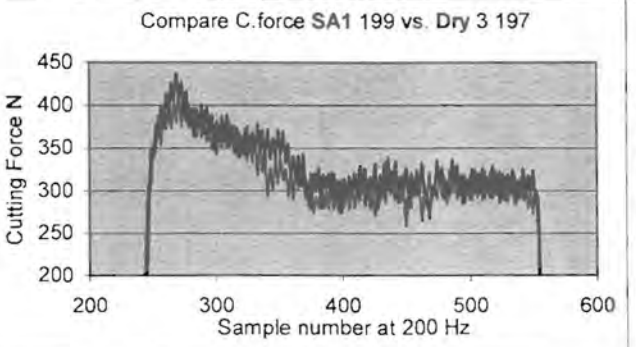

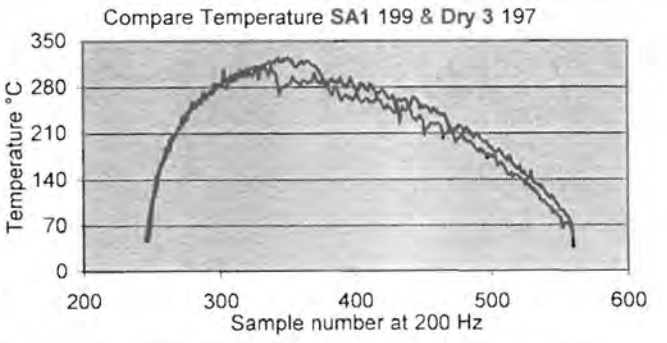

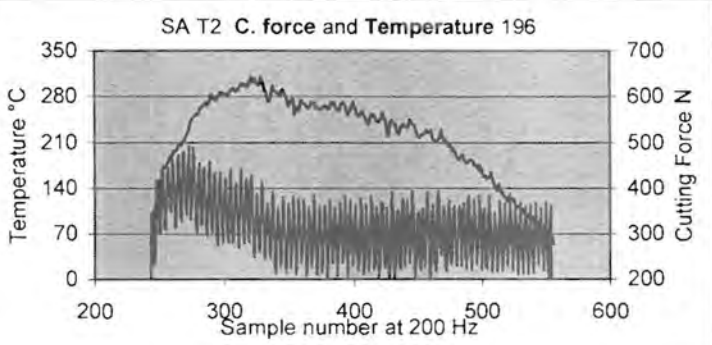

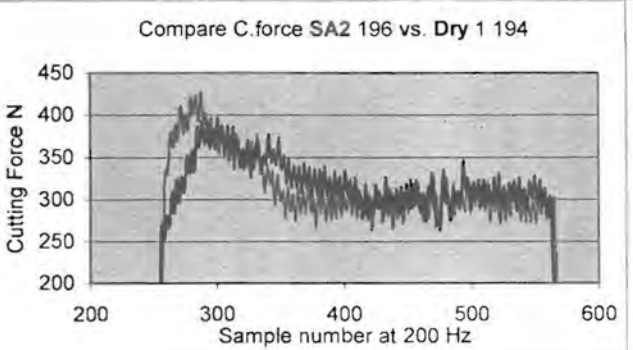

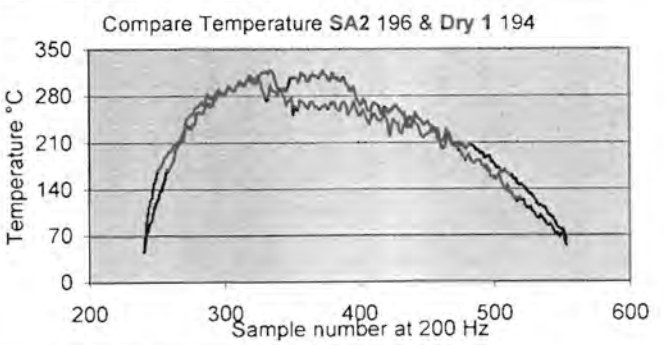

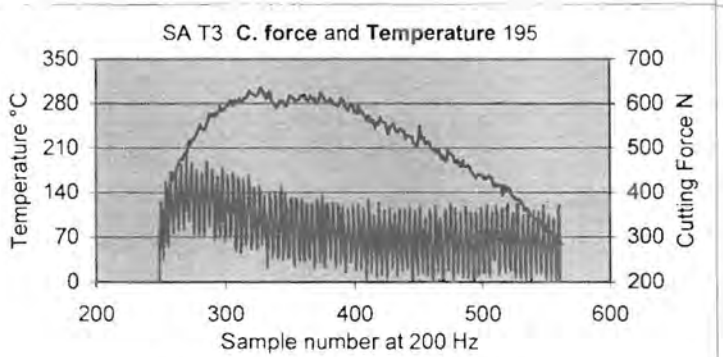

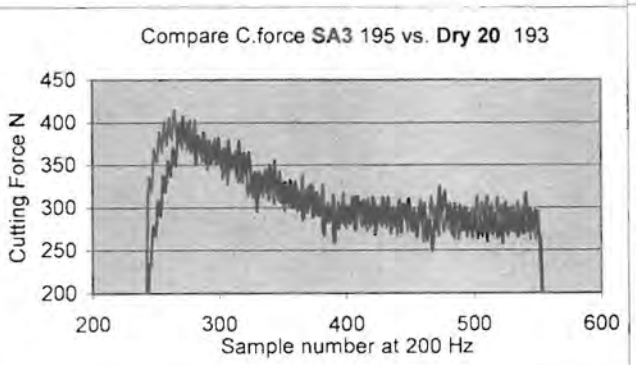

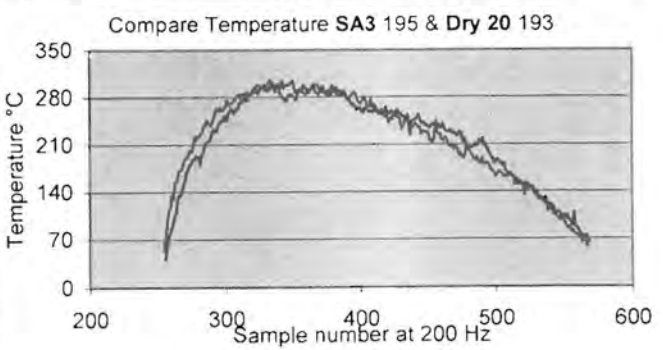

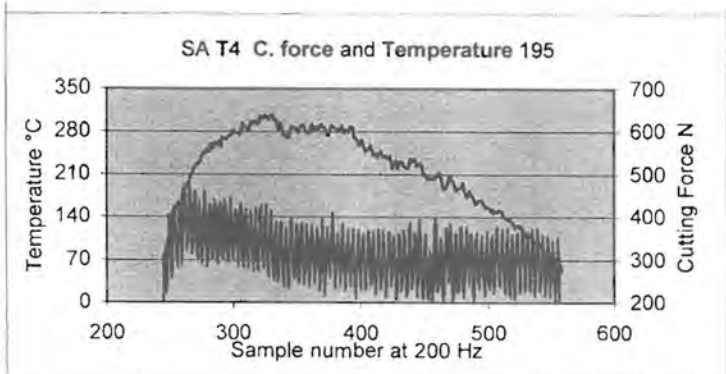
SA T4 C. force and Temperature 195
Temperature °C
Cutting Force N
Sample number at 200 Hz

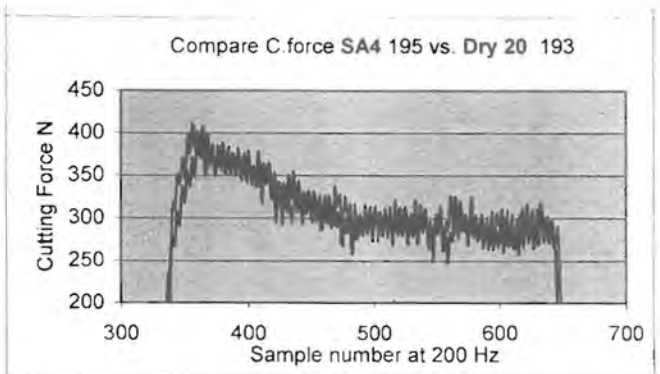
Compare C.force SA4 195 vs. Dry 20 193
Cutting Force N
Sample number at 200 Hz

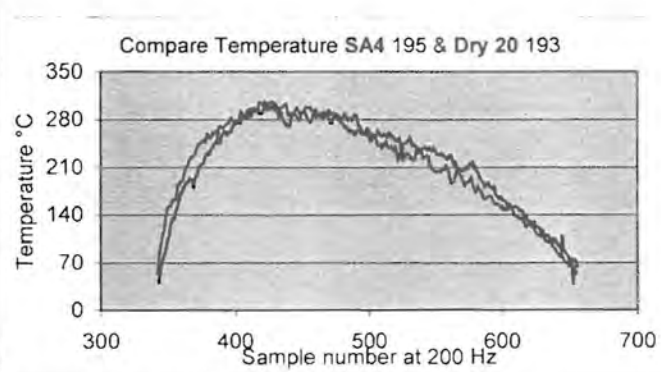
Compare Temperature SA4 195 & Dry 20 193
Temperature °C
Sample number at 200 Hz

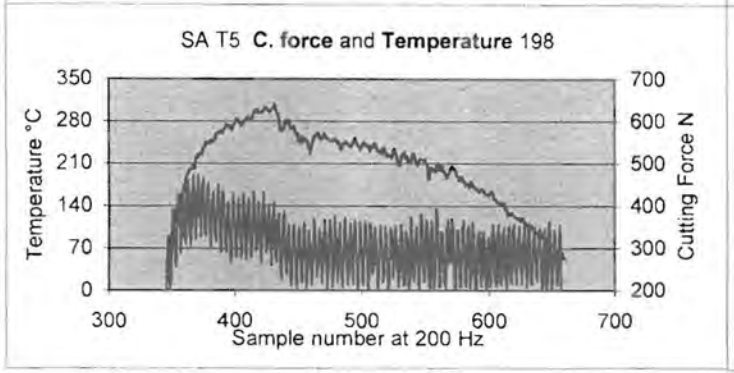
SA T5 C. force and Temperature 198
Temperature °C
Cutting Force N
Sample number at 200 Hz

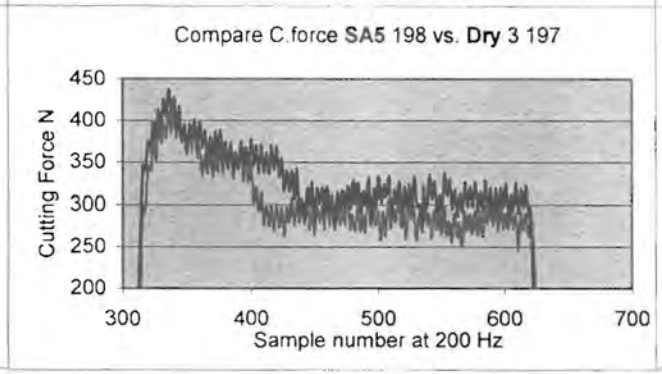
Compare C.force SA5 198 vs. Dry 3 197
Cutting Force N
Sample number at 200 Hz

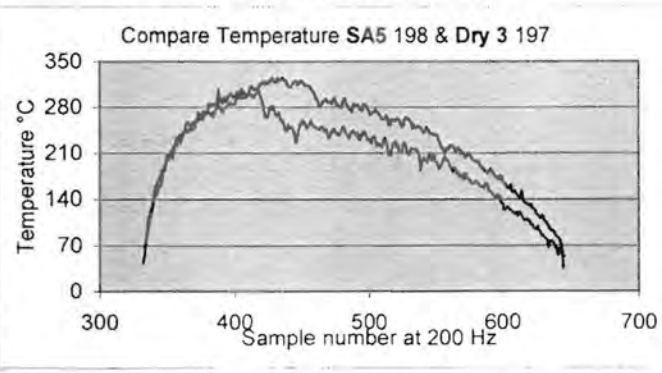
Compare Temperature SA5 198 & Dry 3 197
Temperature °C
Sample number at 200 Hz

Cutting Force and Temperature: raw data

Cutting Force 5 point moving average : Sample and Dry

Cutting Temperature : Sample and Dry

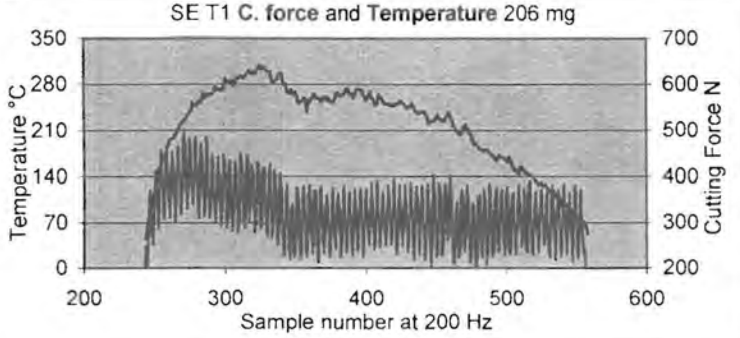

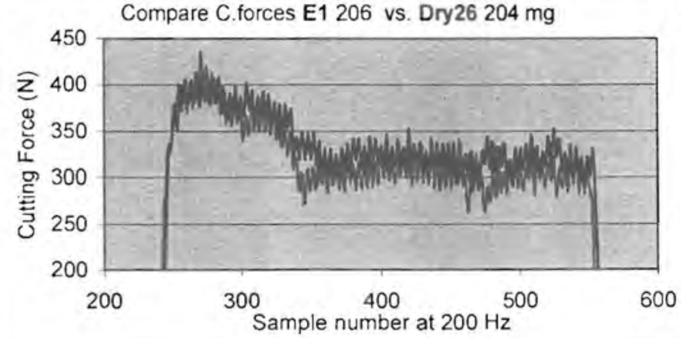

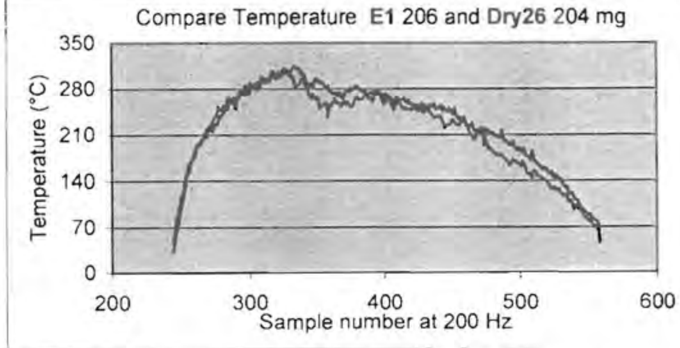

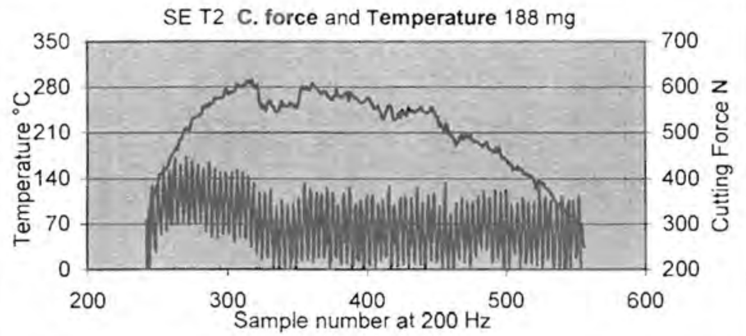

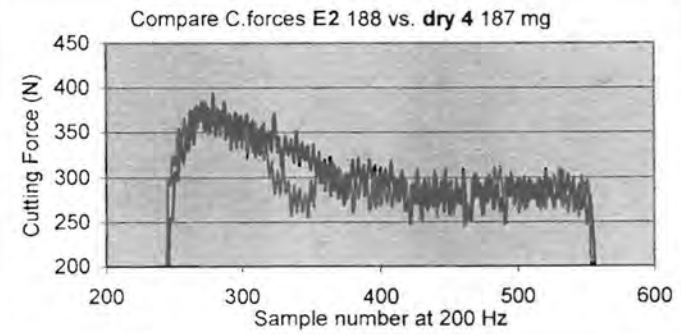

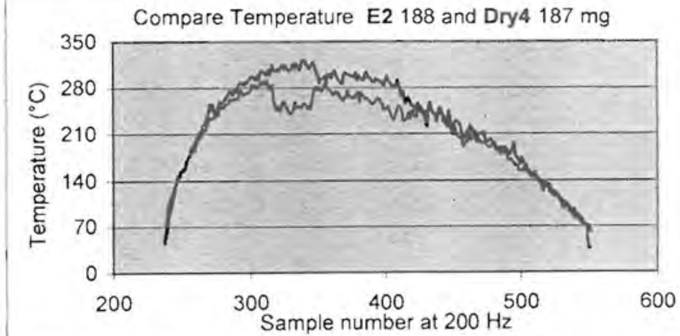

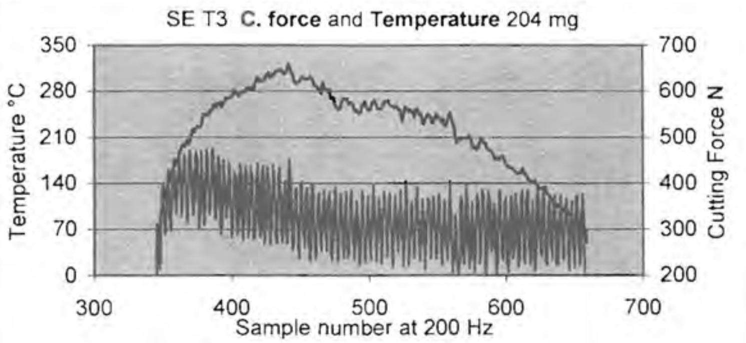

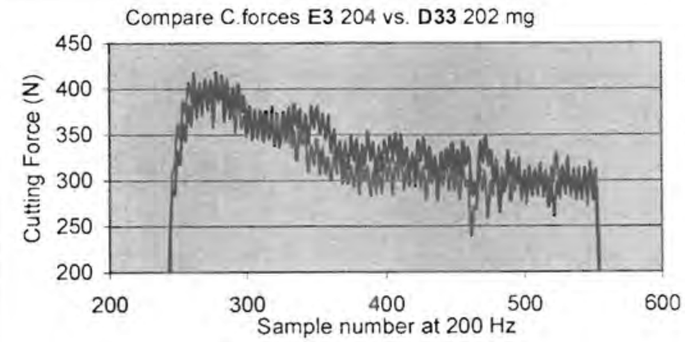

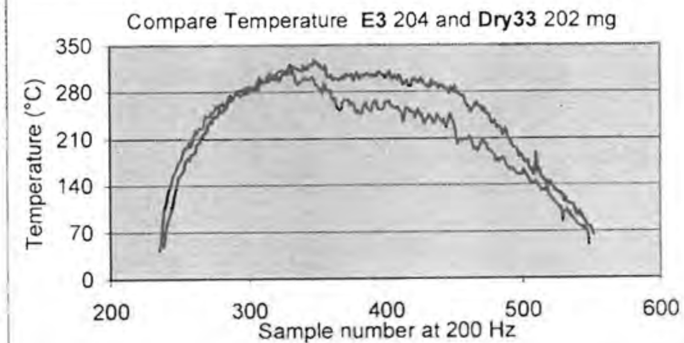

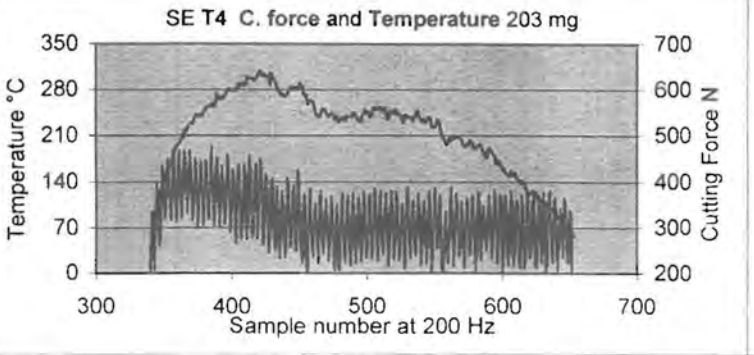
SE T4 C. force and Temperature 203 mg
Temperature °C
Cutting Force N
Sample number at 200 Hz

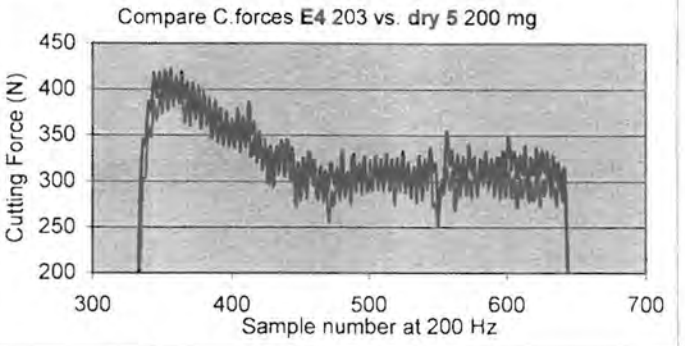
Compare C.forces E4 203 vs. dry 5 200 mg
Cutting Force (N)
Sample number at 200 Hz

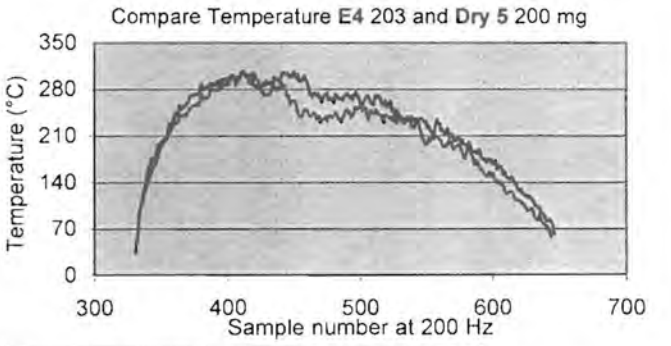
Compare Temperature E4 203 and Dry 5 200 mg
Temperature (°C)
Sample number at 200 Hz

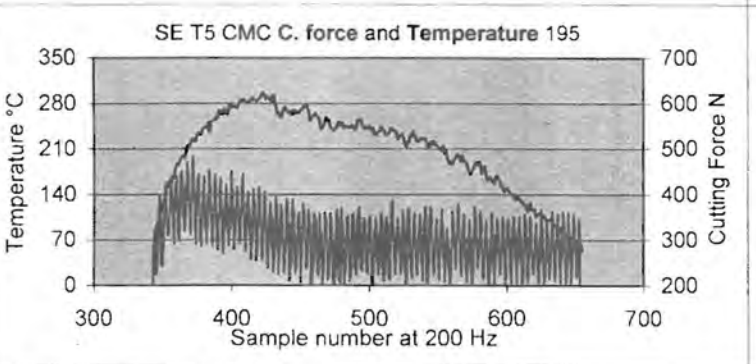
SE T5 CMC C. force and Temperature 195
Temperature °C
Cutting Force N
Sample number at 200 Hz

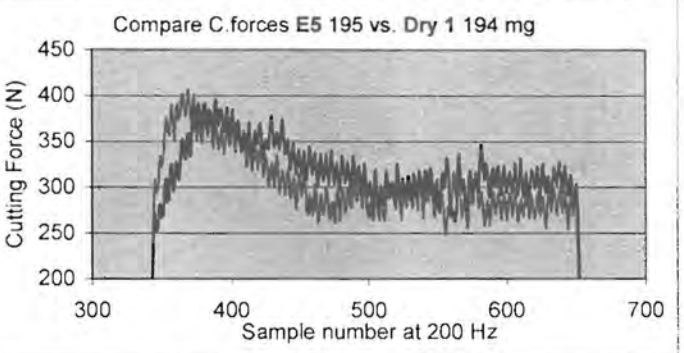
Compare C.forces E5 195 vs. Dry 1 194 mg
Cutting Force (N)
Sample number at 200 Hz

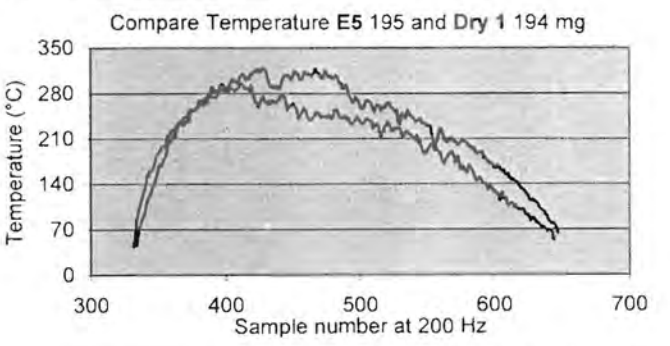
Compare Temperature E5 195 and Dry 1 194 mg
Temperature (°C)
Sample number at 200 Hz

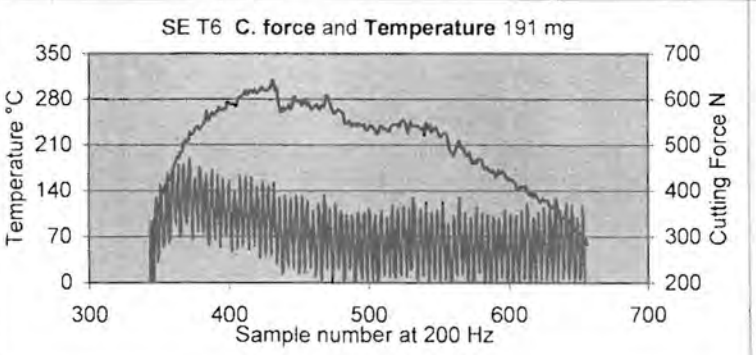
SE T6 C. force and Temperature 191 mg
Temperature °C
Cutting Force N
Sample number at 200 Hz

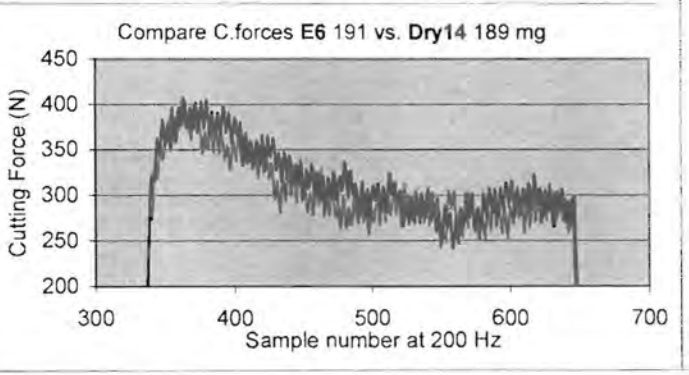
Compare C.forces E6 191 vs. Dry14 189 mg
Cutting Force (N)
Sample number at 200 Hz

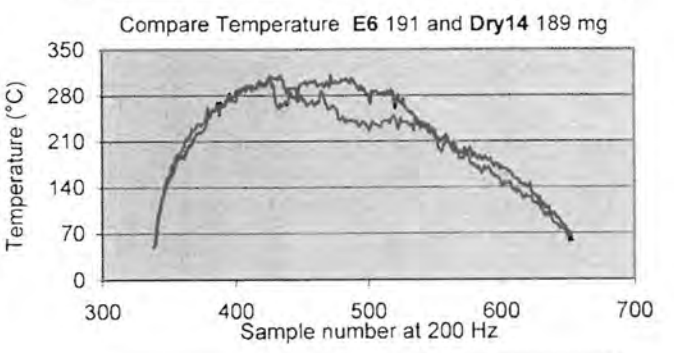
Compare Temperature E6 191 and Dry14 189 mg
Temperature (°C)
Sample number at 200 Hz

Cutting Force and Temperature: raw data	Cutting Force 5 point moving average : Sample and Dry	Cutting Temperature : Sample and Dry
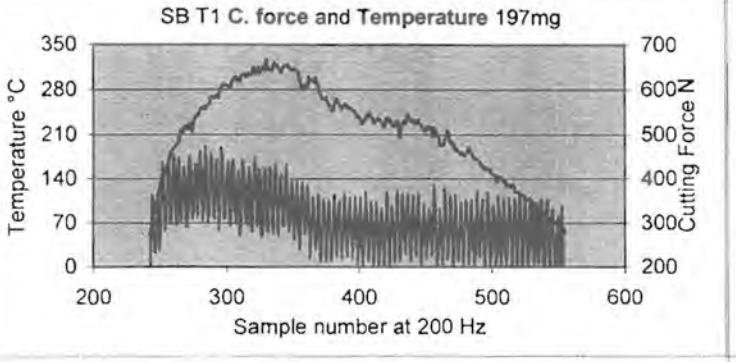	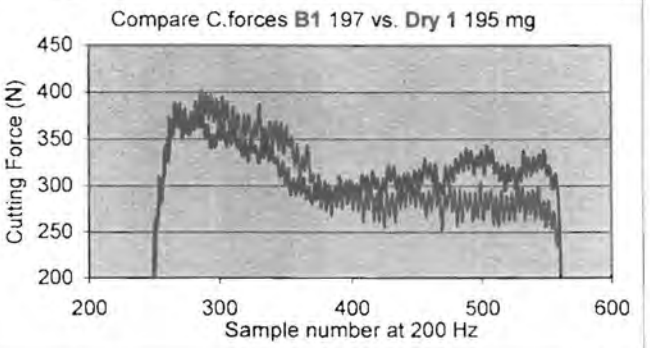	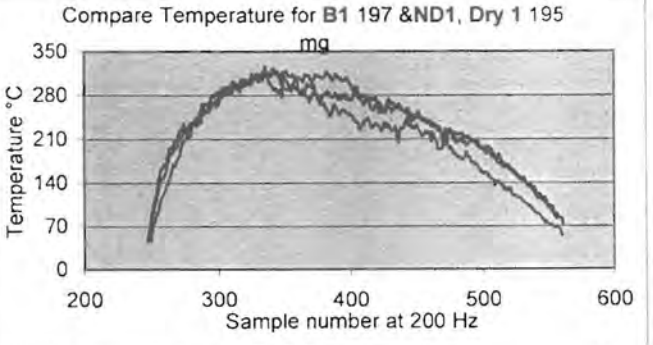
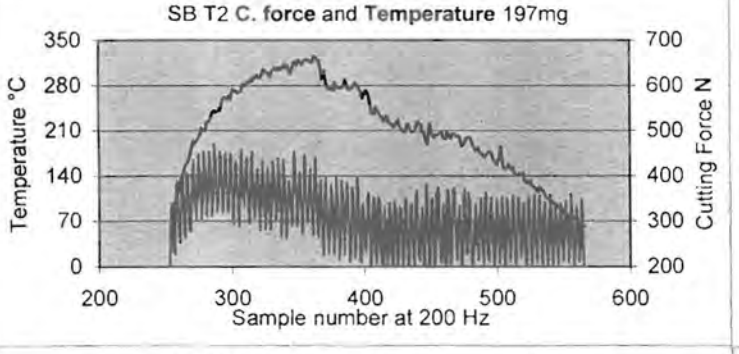	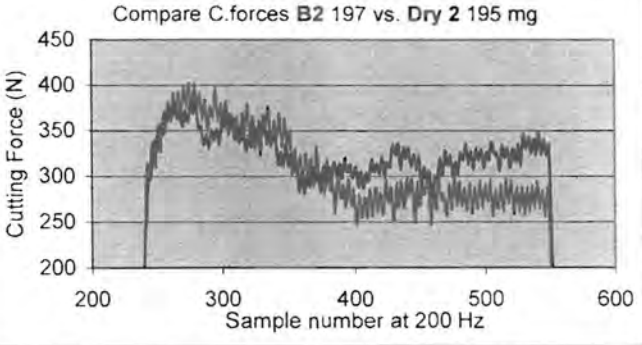	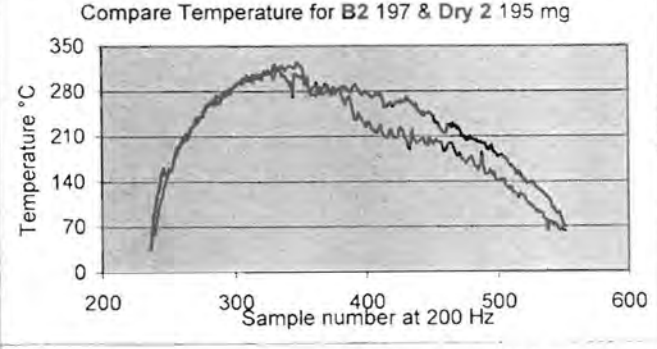
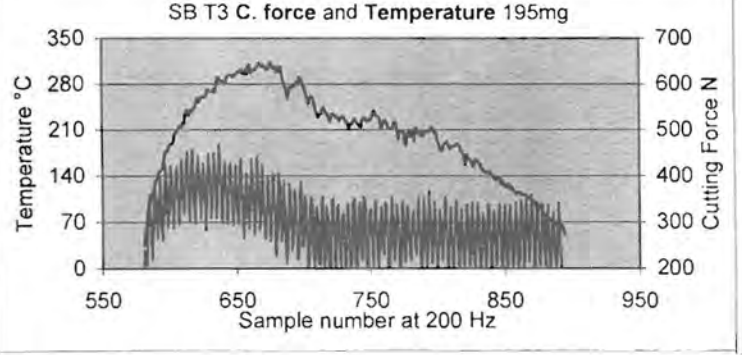	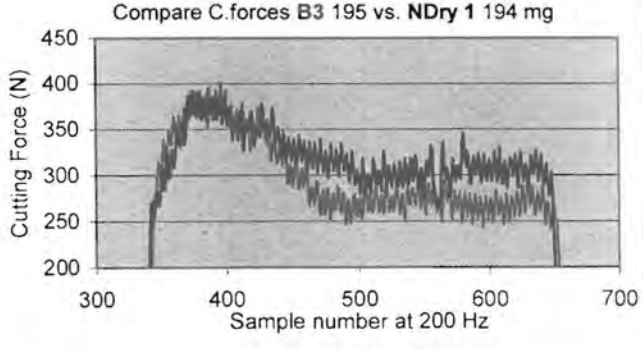	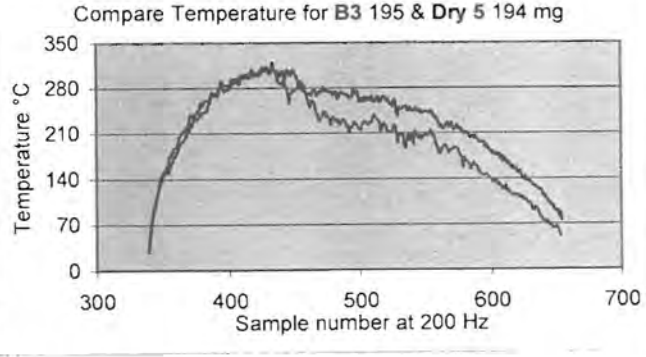

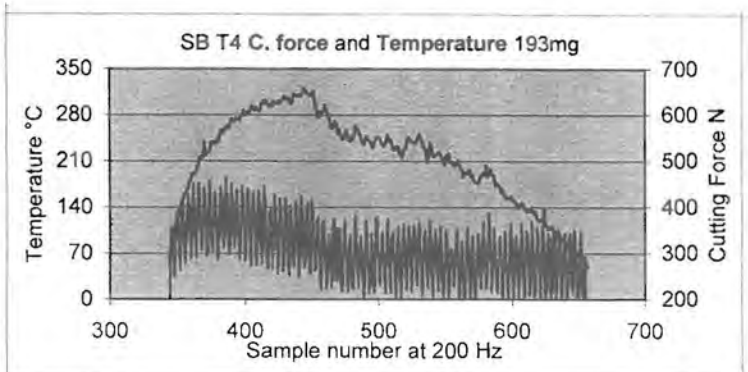
SB T4 C. force and Temperature 193mg
Temperature °C
Cutting Force N
Sample number at 200 Hz

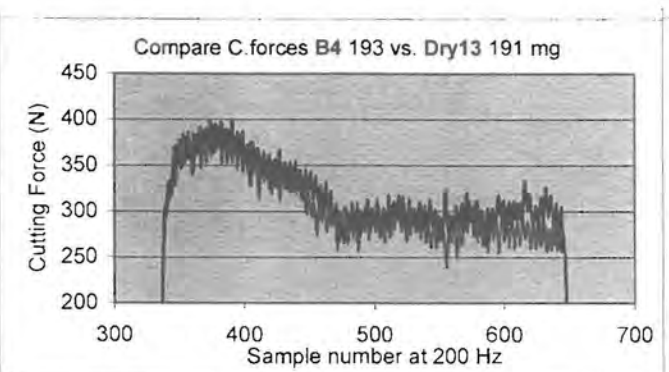
Compare C.forces B4 193 vs. Dry13 191 mg
Cutting Force (N)
Sample number at 200 Hz

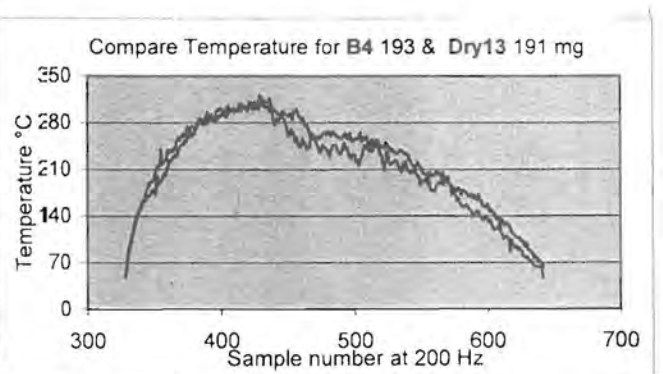
Compare Temperature for B4 193 & Dry13 191 mg
Temperature °C
Sample number at 200 Hz

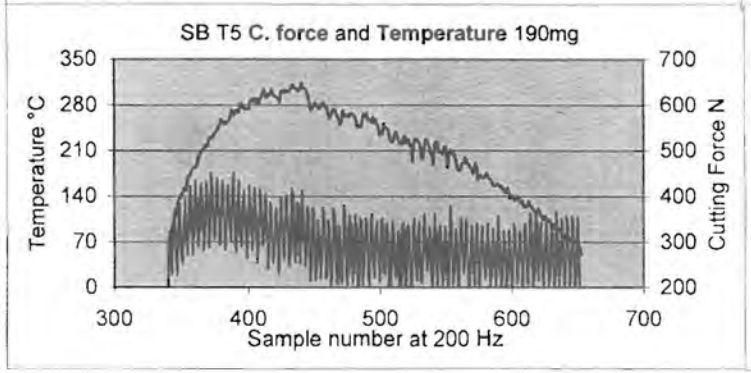
SB T5 C. force and Temperature 190mg
Temperature °C
Cutting Force N
Sample number at 200 Hz

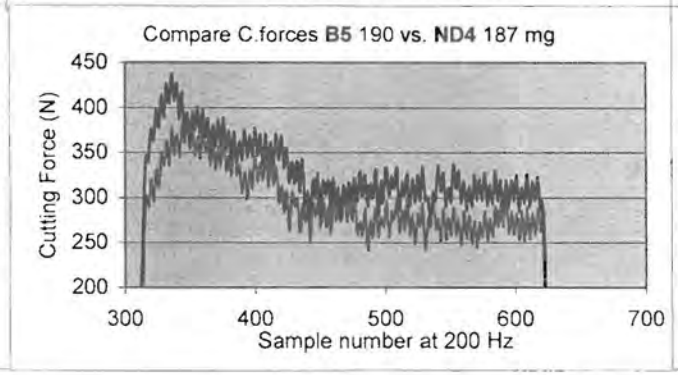
Compare C.forces B5 190 vs. ND4 187 mg
Cutting Force (N)
Sample number at 200 Hz

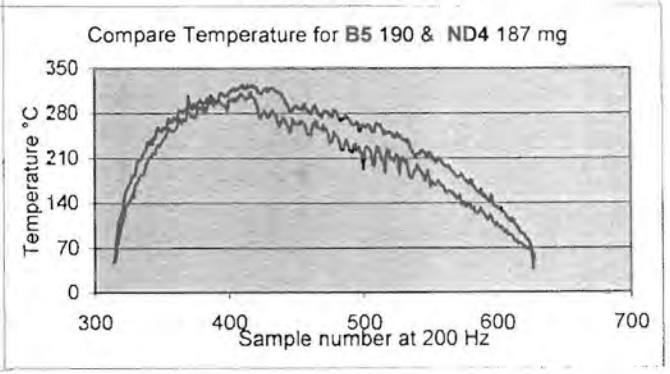
Compare Temperature for B5 190 & ND4 187 mg
Temperature °C
Sample number at 200 Hz

Appendix E:

The output code from the AD/DA card is binary. Direct memory access (D.M.A) is used to transfer data direct from the A/D-byte to memory. Sampling can be done in polled mode or in interrupt mode. For the former the PC is tied up until sampling is completed. For the latter the PC is configured to sample the selected channels independent of direct program control using hardware interrupts and timers. If this mode is used the PC is free for other uses. For the case that the PC exercises control it is tied up anyway because it must continuously output control signals and consequently all operations are performed in polled mode. All the background information for the development of the software for this may be found in the books by Tinker. (Tinker 1996 & 1990)

The binary data are converted to numeric format and the sampled temperature and cutting force data are continuously displayed on screen and dumped to file for later graphical presentation.

To be able to write the software for this case specific operation it is necessary that the EDR software developers kit for Eagle Technology boards be read. Chapter 2 states that EDR60.TPU from c:\EDR\TPAS must be copied to the units directory as EDR.TPU.EDR60 for Turbo Pascal 6.0. The uses EDR statement must then be included in the uses clause in the program for the programmer to have access to the pre-developed software functions, constants and procedures. Similar instructions follow for other programming languages. P3 of the developers kit manual should also be read when taking Eagle cards into use. The newer Eagle cards have different installation instructions than PC30 to PC30D. These are added from the control panel in windows at the applet for add new hardware.

Once this is done programming can start. Follow chapter 3 of the user manual and the EDR_InitBoard procedure description. In summary what is needed to take the board into use is the following: - Call these procedures with their relevant parameters.

1)EDR_AllocBoardHandle(bh); in 7.1 in the manual
2)EDR_InitBoard(bh,baseaddr); in 7.19 in the manual or
2)EDR_InitBoardType(bh,baseaddr,boardtype); 7.20
3)EDR_Set ADInConfig(bh,chan,range,adtype,gain); 7.25
4)EDR_SetDAOutConfig(bh,chan,range,gain); 7.30
5)EDR_GetBoardType(bh,boardtype);

If boardtype in this statement does not reflect your board type you must use the second procedure in 2) above. Consult also appendix A4 in the user manual.

For some cards it is necessary that the jumpers on the board be physically set to correspond to the configuration information specified in 3) and 4) above for the program to function correctly. The user manuals for the relevant cards must be consulted for these settings. When all of the above has been done then program communication between the

process hardware and the PC is open and the other procedures in the manual can be called whenever needed and programming can continue as required.

11. References:

1. Birmingham E., Henshall J.L., Hooper R.M., 1997, "The influence of cutting fluid composition on the wear of high speed steel tools in intermittent cutting", World Tribology Congress, Mechanical Engineering Publications limited P599

2. Boston, O.W. ASME Research Committee, (1952) "Manual on cutting of metals with single-point tools" Second edition published by ASME, P143-150

3. Brown, A. (2002) "Developments in process control monitoring" SA Mechanical Engineer *52* (10), P23-24

4. Considine, Douglas M., (Editor); (1974) Process Instruments & Controls Handbook; McGraw-Hill; 2nd Edition; (P2.23-2.34)

5. de Chiffre L. and Belluco W.,(2002) "Investigations of cutting fluid performance using different machining operations" Lubrication Engineering *58* (10), P22-29

6. du Plessis E. (2001) "The development of limited volume lubrication in metal working operations in South Africa" Seventh International Tribology Conference of the South African Institute of Tribology.

7. Follette, Daniel, (1980) "Machining Fundamentals : A basic approach to metal cutting" Society of manufacturing engineers. P46-55

8. Hill, R., (1950) "Plasticity", Oxford-Clarendon Press

9. Hoffmann Karl, (1989) "An introduction to measurements using strain gauges" Drach Druckerei, Alsbach, Federal Republic of Germany, Hottinger Baldwin Messtechnik GmbH

10. Hutchings I.M, (1992) "Tribology - Friction and Wear of Engineering materials" Edward Arnold a division of Hodder and Stoughton P116, 120-121

11. Kajdas C. (1996) "Tribology – Solving friction and Wear problems" Volume 1 tenth International Colloquium, Technische Akademie Esslingen., P40-45

12. Kelly J.F., and Cotterell M.G., (2002), "Minimal lubrication machining of aluminium alloys", Journal of Materials Processing Technology *120* (1-3), P 327-334 Mechanical and Manufacturing Engineering Department, Cork Institute of Technology, Bishopstown, Cork, Ireland

13. Le Grand R., (1971), "Manufacturing Engineers Manual" McGraw-Hill, (P254-255)

14. Liew W.Y.H., Hutching I.M., Williams J.A., (1997) "Friction and lubrication effects in the machining of aluminium alloys", World Tribology Congress, Mechanical Engineering Publications limited, P337

15. Montgomery, R.S. (1965), "The effect of alcohols and ethers on the wear behaviour of aluminium." Wear *8*, P466-473.

16. Mori S., (1995), "Tribochemical activity of nascent metal surfaces ", proceedings ITC, Yokohama , Satellite forum on Tribochemistry, Tokyo, October 28, 1995, P37-42.

17. Mortier R.M and Orszulik S.T., (1992) "Chemistry and Technology of Lubricants" Blackie Academic and Professional an imprint of Chapman and Hall P45, 217-219

18. Rank Taylor Hobson limited "Surtronic 3 User Manual" Rank Taylor Hobson P5-9

19. Rollason E.C., (1973) "Metallurgy for Engineers" Edward Arnold (P337-340)

20. Rowe, C.N. and Murphy, W.R., (1974), In: Proc. Tribology Workshop. Ling, F.F. (ed.) National Science Foundation, Washington D.C.

21. Tinker, D (1996) "EDR Software developers kit for Eagle Technology boards User manual" Eagle technology
(1990) "User Manual for PC30B/C/D" Eagle Technology

22. Trent E.M., (1977) "Metal Cutting" Butterworths

23. Van der Voort, George F., (1999), "Metallography, principles and practice." Mc Graw-Hill P196-198, 350-353

24. Van der Waal, G, (1985) "The relationship between chemical structure of ester base fluids and their influence on elastomer seals and wear characteristics" Journal of synthetic lubrication *1* (4) P281

25. Varadarajan A.S., Philip P.K. and Ramamoorthy B., (2001), "Investigations on hard turning with minimal cutting fluid application (HTMF) and its comparison with dry and wet turning", International Journal of Machine Tools and Manufacture *42* (2), January 2002, P 193-200, Manufacturing Engineering Section, Department of Mechanical Engineering, Indian Institute of Technology, Madras, Chennai, 600036, India

26. Vieira J.M., Machado A.R., and Ezugwu E.O., (2001) "Performance of cutting fluids during face milling of steels' Journal of Materials Processing Technology *116* (2-3), P 244-251

27. Xuegang M., Yangshan S., Feng X., Wenwen D. and Wu D., (2002) "Analysis of valence electron structure (VES) of intermetallic compounds containing Mg-Al-based alloys" Materials,Chemistry and Physics *78* (1) P88-93
Department of Material Science and Engineering, South E. University, Nanjing, China, 210096

28. Zorev N.N, Massey H.S.H.and Shaw M.C,. (1966) "Metal Cutting Mechanics " Pergamon Press London, P273

Web site references:

29. ARTX, (2002) Vortex tube coolers, http://www.artxltd.com, [2002, April 4]

30. Capgo, (2002) Software reference compensation, www.capgo.com, [2002, October 9]

31. Clark, J. (2002) Chemguide helping you to understand chemistry, http://www.chemguide.co.uk/atoms/bonding/metallic.html, [2002 October 29]

32. Nix, Roger (2002) An introduction to surface chemistry, http://www.chem.qmw.ac.uk/surfaces/scc, [2002 May 5]

33. Fox Valley Technical College (FVTC), (2000) Cutting fluid types and uses, http:\\its.foxvalleytech.com, [2002,April]